Simultaneous Synthesis and Optimization of Refrigeration Cycles and Heat Exchangers Networks

Matteo Martinelli[a], Cristina Elsido[a], Ignacio E. Grossmann[b], Emanuele Martelli[a*]

[a] *Politecnico di Milano, Dipartimento di Energia, Via Lambruschini 4, Milano, IT*

[b] *Department of Chemical Engineering, Center for Advanced Process Decision-Making, Carnegie Mellon University, Pittsburgh, PA, USA*

* emanuele.martelli@polimi.it

Abstract

This work proposes a simultaneous approach for the synthesis and design optimization of refrigeration cycles integrated with heat exchanger networks. The methodology includes a novel refrigeration cycle superstructure capable of reproducing a wide range of cycle architectures and an effective solution algorithm (based on the decomposition of the problem on two levels) to tackle the challenging Mixed Integer Non-Linear Program. In addition to optimize the cycle and heat exchanger network structure, the methodology can optimize cycle pressures and temperatures (including superheating and subcooling degree of the working fluid in the refrigeration cycle). The application to four literature case studies indicate that the proposed approach returns solutions which are considerable better in terms of economics than those published in literature (up to 40% decrease in total annual cost).

1. Introduction

The design of a refrigeration cycle represents a challenging task, mainly due to the wide range of schemes and working fluid alternatives, resulting from the evolution of this technology during the last 100 years. All these possible alternatives have been developed to meet the needs of different applications, such as industrial refrigeration, heat pumps for industrial waste heat recovery and cryogenic applications like natural gas liquefaction. Thus, the optimal design of refrigeration cycles calls for the development of systematic optimization approaches capable of exploring all the alternative configurations and finding the best trade-off between cost and performance.

Many authors in the literature have addressed the optimization of refrigeration cycles, but to the best of the author's knowledge only a few considered a combination of technical, thermodynamic and economic parameters in the process. In the study by Wallerand et al. [1], a comprehensive literature review is made considering all the studies from the seventies. The main approaches adopted for optimization are three:

- Pressure and temperature optimization approach: a case-related structure is created ad-hoc for the study, and then optimization is performed. In this situation the optimization options are reduced to the levels of pressure/temperature selection with a forced structure. This approach does not involve binary variables for components selection, the structure is already defined.

- Synthesis approach: a general structure of a refrigeration cycle is replicated for a certain number of levels, then an algorithm iterates looking for the best possible solution in terms of the selected optimization driver.
- Synthesis approach based on reduction: a very complex superstructure containing all the technical possibilities is generated and then the optimum solution is found selecting only a portion of this superstructure, based on the chosen optimization drivers. Synthesis approaches allow to define also the optimal structure, together with temperatures and pressures.

The first approach is the one followed by Alabdulkarem et al. [2], where the optimization is based on an iterative procedure, assuming a priori the number of stages and their structure and calculating for a selected range of pressures the corresponding liquefaction temperature and the heat and power duties involved in the cycle to obtain the COP (coefficient of performance) of the cycle. Baakeem et al. [3] maximized the coefficient of performance (COP) of multistage vapor-compression refrigeration cycle by optimizing the cycle variables (pressures, temperatures) using the Conjugate Directions Method. Nasruddin et al. [4] tackles the multi-objectives optimization of a cascade refrigeration system using refrigerant C_3H_8 in high temperature circuits and a mixture of C_2H_6/CO_2 in low temperature circuits. Key cycle variables are optimized in a bi-objective optimization approach minimizing the total annual cost and the total exergy destruction. Eini et al. [5] proposed a similar multi-objective approach considering minimum cost, maximum efficiency and minimum quantitative risk assessment index.

One of the first examples of synthesis approach for refrigeration cycles is the one proposed by Shelton and Grossmann [6], [7]. A general super-structure is postulated and then replicated for a number of discretized temperature intervals, representing the basic refrigeration cycle, with condensation only at the upper level, evaporation only at the lower and, connecting the levels, direct contact coolers/separators with intercoolers and intermediate loads. Once the structure is selected, the problem is formulated, and can then be solved. On the other hand, this method lacks in considering all the technological solutions (such as subcooling and superheating), and it makes linear approximations to avoid non-linearities. For example, heat exchanger cost is calculated only after the optimization, and a minimum ΔT approach is followed in the solution: no optimization is performed on temperature differences.

Marechal and Kalitventzeff [8] proposed a method for the optimal synthesis of refrigeration cycles, based on a three-step procedure: temperature levels selection, refrigerant selection and MILP optimization of structure.

Hasan et. al [9] focused on the use of refrigeration cycles for LNG liquefaction, with a model based on a MINLP formulation optimizing the compression chain in terms of power consumption. Kamalinejad et al. [10] proposed a superstructure-based optimization procedure for cascade systems, with exergy-based analysis for optimal pressure level selection and a MINLP formulation minimizing compression power instead of TAC. Exergy analysis is combined with pinch analysis for refrigeration cycles optimization for LNG purpose in Ghorbani et al. [11]. In Yang et al. [12], also HEN superstructure optimization is considered; the objective is again compression power minimization, thus ignoring economic aspect of optimization.

Zhang et. al [13] proposed a methodology based on a MINLP formulation for the integration of absorption refrigeration cycles in industrial network for low grade heat recovery, with particular focus on the HEN structure. Olueye et. al. [14] developed a method for heat pump integration in existing plants for heat recovery purpose. The model is a MILP, considering TAC minimization as objective function.

Wallerand et al. [1] proposed a method optimizing both capital and operating expenses. In a very complex super-structure (reduction approach), the main technological solutions can be selected. The

proposed formulation is a MINLP, solved with a master-slave architecture where temperatures and pressures are selected at the master level, while the size and existence of the utilities are selected at the lower level. In order to focus on the optimization of the refrigeration cycle the method does not rigorously perform the optimization of the HEN, the areas of the exchangers are approximated by calculating with precision only the overall surface and not the single exchangers ones. Moreover, no optimization is performed on the ΔTs and HEN structure, negatively affecting the possibilities of the model to deal with heat integration.

Some models were designed specifically for cascade cycles synthesis. The search for optimal synthesis is not a recent problem. King and Barnes [15] proposed a method based on dynamic programming, where the structural alternatives were expressed as nodes, connected by path identified by a value of cost; in this way the problem becomes a minimum-cost path one. Colmenares and Seider [16] proposed an NLP formulation for the optimization of cascade cycles, considering both compression and utility in the objective function. HEN integration is evaluated with a minimum temperature approach, and different candidate refrigerants are considered. In Vaidyaraman and Maranas [17] a methodology based on TAC (thus considering all cost components) partially increasing the possible technological solutions and allowing fluid selection optimization is proposed: in this super-structure, also economizers can be selected as an alternative to pre-saturators (direct contact coolers/separators), still in a single-level structure replicated many times. The model is again an MILP, since linearizations are made; in this case, they are led to weaker approximations because perfect gas is assumed. More Recently, Dinh et al. [18] based the design of superstructure on exergy analysis. The formulated model including the HEN is an MILP, but again no economics are considered.

Yet, none of these approaches combined all the main optimization targets in one method, considering compression refrigeration cycle structure and pressures/temperatures, HEN structure, thermodynamic and economic aspects. For this reason, the objective of this work is to develop a model able to consider several technical possibilities available for compression refrigeration, and selecting the best ones for the selected purpose. In particular, the model considers:

- All the main architectures of compression refrigeration cycles proposed for pure refrigerant fluids
- The optimal configuration of the HEN (Heat Exchanger Network): not only the general structure of the cycle but also the heat integration both with utility and process hot and cold streams, which means coupling in the best possible way hot and cold streams to guarantee a required refrigeration duty (and if necessary heating too).
- The optimization of thermodynamic properties, choosing the best temperature and pressure for condensations and evaporations, optimal heat exchange temperatures and selecting the optimal values for all the technical solutions (sub-cooling, super-heating etc.).

This is done combining a refrigeration cycle superstructure with a HEN superstructure and considering their thermodynamic properties as variables to be optimized minimizing TAC (Total Annual Cost).

The method proposed here focuses on pure-refrigerant cycles, but it can be easily extended to mixed-refrigerant cycles.

2. Problem statement and methodology

The problem addressed in this work is relevant for the design of the heat recovery system of industrial process requiring the integration of heat pumps or refrigeration cycles. The problem can be summarized as follows.

"Given a set of hot and cold process streams with given mass flow rates, inlet and outlet temperatures, and a set of possible hot/cold utility systems (e.g., boilers, cooling water), the superstructure of possible reverse Rankine cycle configurations, determine the optimal selection of utility systems, the design of the reverse Rankine cycle (selection of pressure levels, mass flow rates of each utility stream, temperatures at inlets and outlets of the evaporator/condenser/intercoolers, etc.), the HEN between process–process as well as process-utility, process-cycle and cycle–utility streams, minimizing the Total Annual Cost (TAC, sum of annualized capital cost and yearly operating costs) of the overall system (utility systems, reverse Rankine cycle and HEN)".

Following the approach proposed by Elsido et al. [19],[20] for organic Rankine cycles and steam cycles, the basic idea is to adopt the "Synheat" superstructure by Yee and Grossmann [21] for the HEN and include the streams of the refrigeration cycle superstructure as hot/cold streams with variable mass flow rate. As for the refrigeration cycle superstructure, the *p-h superstructure* originally proposed by Elsido et al. [22],[23] for power cycles is adapted and extended here for refrigeration cycles. In particular, the superstructure of the compression refrigeration cycle is modelled as a series of *headers* representing thermodynamics conditions (i.e., points in the *p-h* diagram), connected by streams and components (valves, compressors, heat exchangers, mixers, splitters).

In Figure 1 the colouring code that will be used in the paper figures is reported.

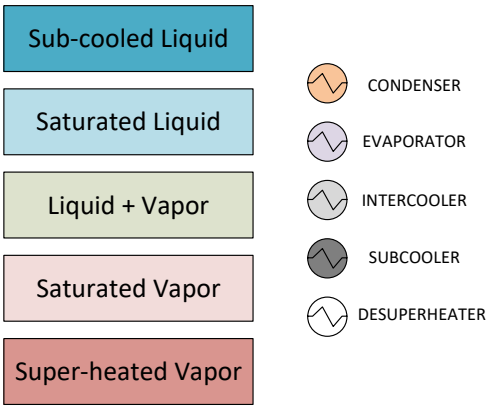

Figure 1. Colouring Code for Headers (rectangles on the left) and Heat Exchangers (on the right)

Two versions of the methodology will be presented:

- Fixed p and T of Headers optimization: the refrigeration cycle and HEN structure are optimized with fixed thermodynamic conditions of the cycle headers (fixed T and p) and the resulting nonconvex MINLP is solved with the bilevel decomposition algorithm presented in Elsido et al. [19].
- Variable p and T of Headers optimization: also the pressures and temperatures of the refrigeration cycle are optimized and the resulting MINLP is optimized with an extended version of the bilevel decomposition algorithm.

The mathematical model is formulated under the following assumptions: i) constant specific heat capacities; ii) constant heat transfer coefficient for each stream; iii) counter-flow arrangement for all heat exchangers; iv) isothermal mixing assumption for the HEN superstructure (i.e., within the HEN the stream branches exit each stage at the same temperature and are mixed before entering the subsequent stage).

3. Reverse Rankine Cycle Superstructures

The two versions of the methodology require different refrigeration cycle superstructures, as described in the following subsections. Indeed, compared to the superstructure developed for "Variable p and T of headers optimization", the superstructure for the "fixed p and T of headers" model needs to employ multiple headers with different degrees of condenser subcooling and evaporator superheating.

3.1 Reverse Rankine cycle superstructure for optimization with fixed p and T of headers

In Figure 2 the superstructure obtained by considering all the main available technological solutions is shown. The basic structure has been replicated for three pressure levels for simplicity reasons, namely three being the minimum number of levels necessary to show all the possible cycle configurations. In the case studies a superstructure with more levels will be used. The conditions of the headers are reported on the p-h diagram of Figure 3 assuming to use R134a as working fluid.

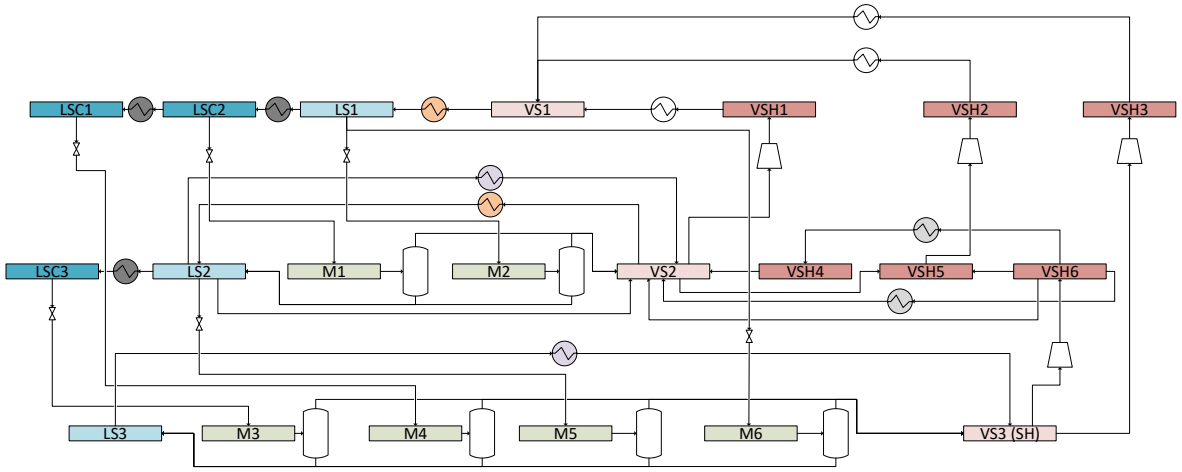

Figure 2. General Compression Refrigeration Cycle Superstructure with 3 Pressure Levels

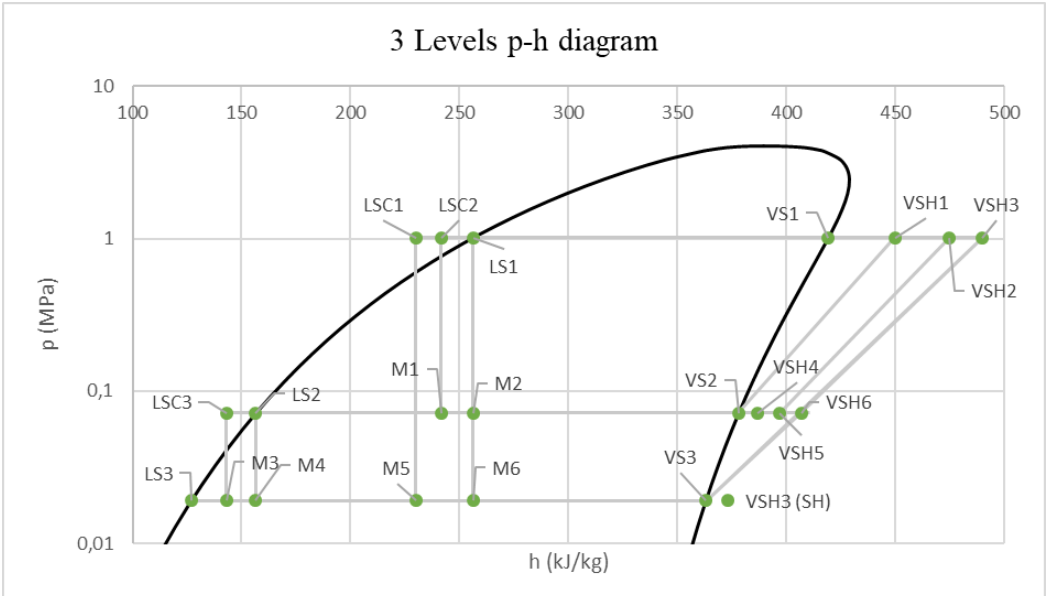

Figure 3. p-h Diagram of the 3 Levels Superstructure

The general *p-h* superstructure can reproduce all the main cycle schemes adopted in the industry, as shown in the following examples:

- Simple Refrigeration Cycles (see Figure 4): basic configuration of the technology, typically used when small temperature differences have to be reached (e.g., domestic refrigerators). In the cycle in figure, saturated vapour *VS1* is condensed, and the obtained saturated liquid *LS1* is then throttled. The result is a two-phase flow leaving the valve. For the sake of modelling, the two-phase stream leaving the valve is decomposed in the liquid fraction and vapor fraction. Only the liquid fraction *LS2* is evaporated (so it takes part to the HEN), while the vapour fraction *VS2* can go directly to compression. The result of compression is superheated vapour *VSH1*. Since the HEN superstructure can include only streams with constant heat capacity, the condenser is split into a de-superheater and a condenser section.

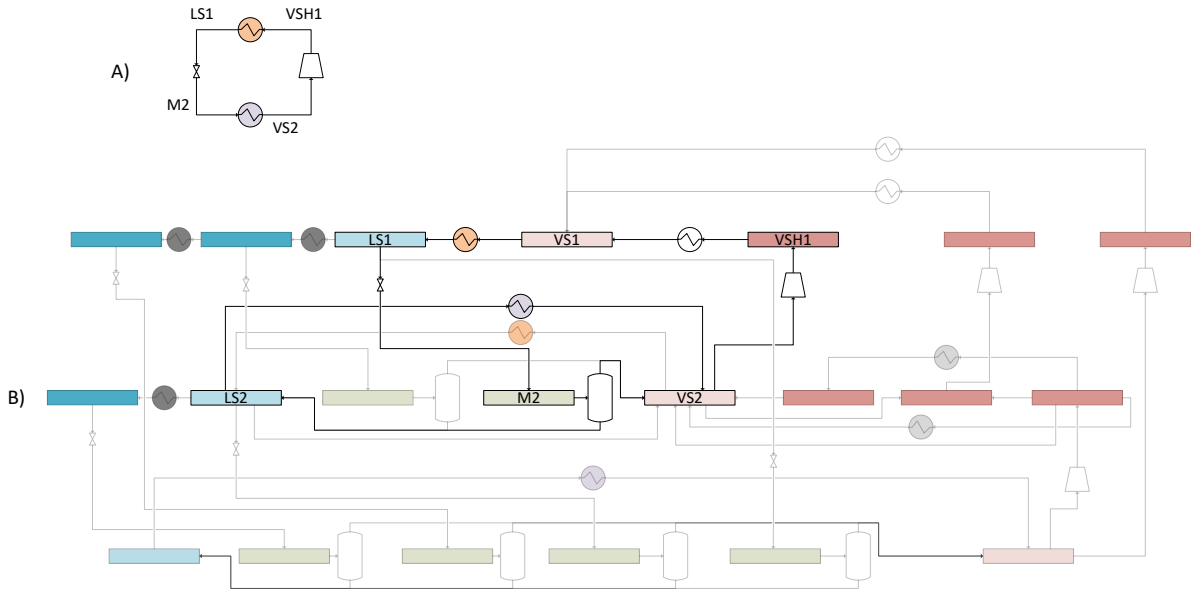

Figure 4. Part (A) Scheme of a simple single-level refrigeration cycle; part (B) representation of the simple refrigeration cycle in the general *p-h* superstructure.

- Refrigeration Cycles with double throttling (see Figure 5). These cycles feature two throttling valves (one from LS1, the other one from LS2), a vapor-liquid separator at intermediate pressure (from header M2) and a compressor with two stages/groups (here referred to as "low pressure" and "high pressure" stages). The basic idea is to avoid throttling the vapor which exits the first expansion valve (in header M2), and sending it directly to the inlet of the high-pressure compressor (header VS2). This allows saving compression power of the low-pressure compressor without affecting the cooling power absorbed by the evaporator (since the vapor separated in M2 would not contribute absorbing any evaporation enthalpy within the evaporator). Thus, the saturated liquid at intermediate pressure is collected in header LS2 and sent to the second throttling valve which discharges a two-phase flow (M5). For the sake of convenience in modelling the evaporator HX within the HEN synthesis superstructure, the two-phase flow is virtually separated into the flow of saturated liquid (LS3) crossing the evaporator, and the flow of saturated vapor sent directly to the saturated vapor header (VS3). Since the outlet of the low-pressure compressor is superheated vapor (VSH6) and the header VS2 is required to be saturated vapor by assumption (this assumption can be removed in the model proposed in Section 2.2), a small flow of liquid vapor needs to be extracted from LS2

and mixed in VS2. The energy and mass balance equations of the Rankine cycle model optimizes the liquid flowrate as well as all the other stream flowrates.

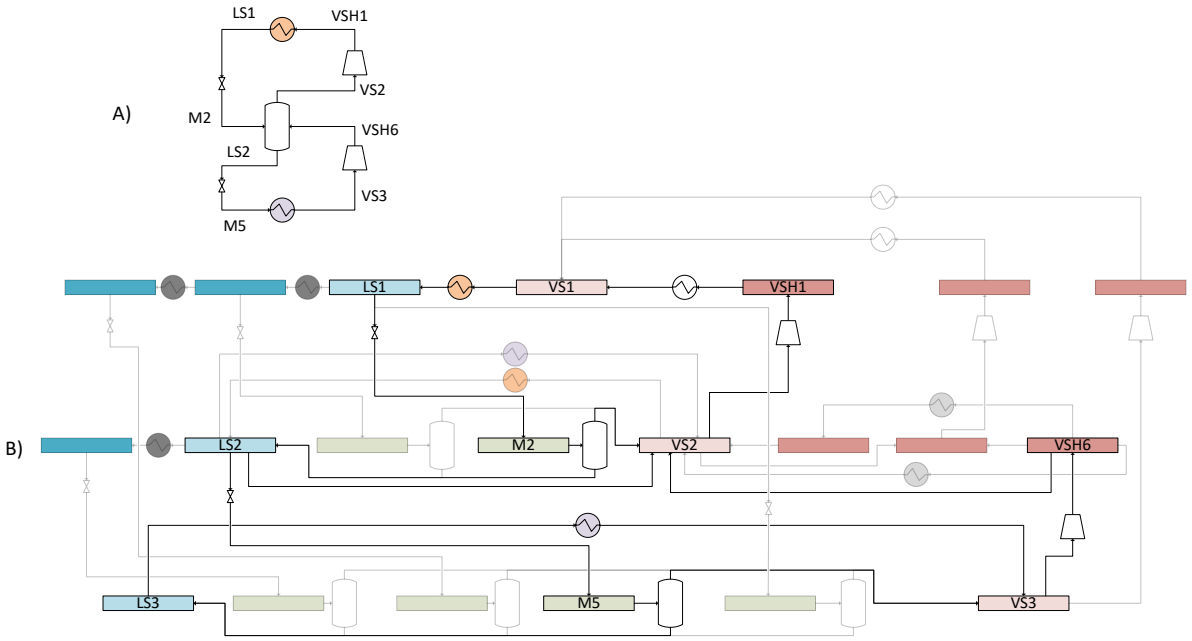

Figure 5. Part (A): scheme of a double-throttling refrigeration cycle with single pressure levels of evaporation and condensation; Part (B) representation of the double-throttling refrigeration cycle in the general *p-h* superstructure.

- Refrigeration Cycles with multiple options for compressor intercooling. Figure 6 shows the scheme of a refrigeration cycle with single level of evaporation and condensation, optionally double-throttling, and 4 different options for compressor intercooling typically adopted in industrial applications to decrease the compression power. In option A, superheated vapour resulting from compression *VSH6* is partially cooled down to *VSH4* (still superheated) by the cooler "A". If option B is selected, the cooler "B" is activated to reach saturated vapour condition (header *VS2)*. In option C, superheated vapour *VSH6* is partially cooled down to *VSH5* (still superheated) by mixing with saturated vapour *VS2 (*vapour-mixing intercooling). In option D, intercooling happens by direct mixing with the saturated vapor and some saturated liquid leaving the high-pressure throttling valve. It should be noted that in this configuration, the represented flash tanks may have different meaning depending on the selected option: if solutions A) or D) are selected, the tank acts as direct contact cooler and separator, on the other hand with solutions B) and C) the tank just acts as a separator.

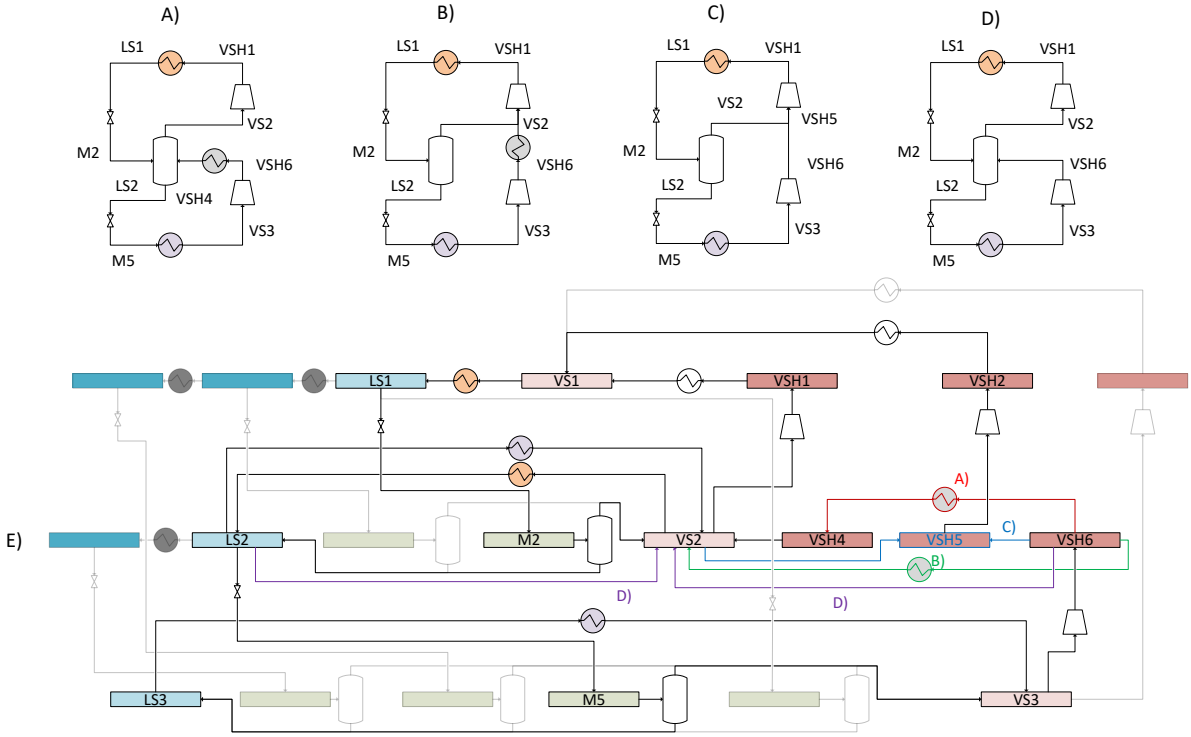

Figure 6. Part (A): scheme of double-throttling reverse Rankine cycle with intercooling option A; Part (B): scheme of double-throttling reverse Rankine cycle with intercooling option B; Part (C): scheme of double-throttling reverse Rankine cycle with intercooling option C; Part (D): scheme of double-throttling reverse Rankine cycle with intercooling option D; Part (E): representation of the different compressor intercooling schemes by the Rankine cycle superstructure (red = option A, green = option B, blue = option C, purple = option D).

- Refrigeration cycles with multiple evaporation and condensation levels. Adopting multiple condensation or evaporation levels is recommended when dealing with hot/cold process/utility streams requiring cooling/heating power over a wide range of temperatures. For simplicity they are represented by two evaporation levels and one condensation level. It should be noted that, being the structure connected as seen in part (B) of Figure 7, the intermediate pressure evaporator can act both as an actual evaporator (line LS2 - VSH5) or as

an intermediate load (line M2 - VS2), evaporating only a portion of the mixed flow coming from the throttling valve.

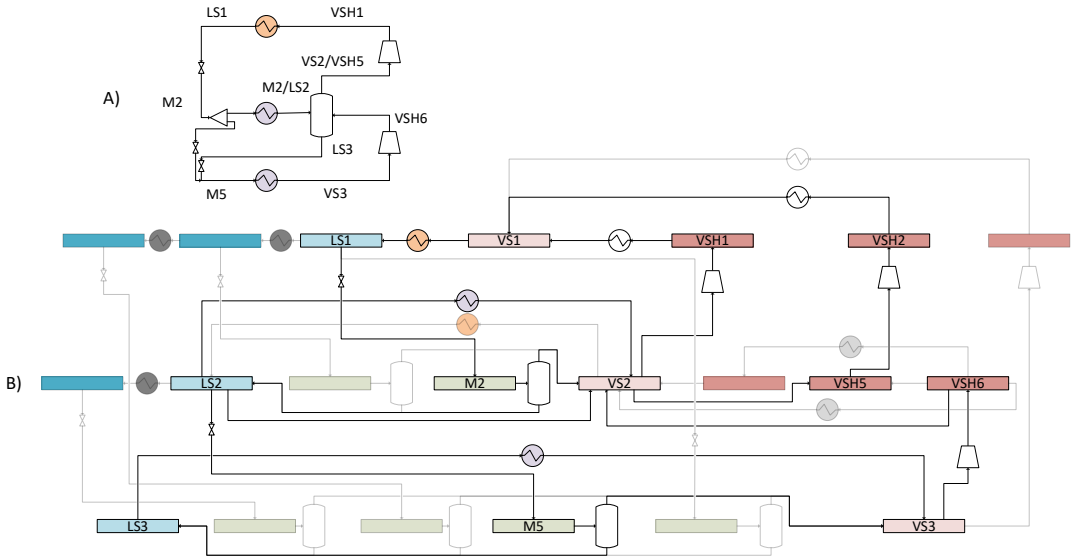

Figure 7. Part (A): Example of cycle with 2 evaporation and 1 condensation levels; Part (B) representation of the cycle in the general p-h superstructure.

- Liquid Sub-Cooling at condenser outlet and vapor Super-Heating at evaporator outlet. These two components can be used to increase the thermal power absorbed by the evaporator and, as a consequence, the COP. Their optimal values depend on the temperature profile of the cold stream to be heated by the condenser, and that of the hot stream to be cooled down by the evaporator. In this version of the superstructure, subcooling and superheating degrees are discretized in order to deal with fixed temperature headers. The simplest cycle involving subcooling is represented in Figure 8: saturate liquid *LS1* is cooled down to *LSC2* conditions before being throttled to the lower level: again, a separator must be used to model the two-phase flow whose liquid fraction is evaporated, while vapour is sent directly to compression. As for superheating, it is worth noting that considering several headers of superheated vapor at the exit of the evaporator interconnected by superheaters would lead to a large increase in the model complexity. For this reason, the optimization of the superheating degree is performed by means of a sensitivity analysis using a single superheated vapor header, as shown in Figure 9. The scheme is the same as a simple refrigeration cycle, where a different condition is reached at the outlet of the condenser (subcooled liquid) or the evaporator (superheated).

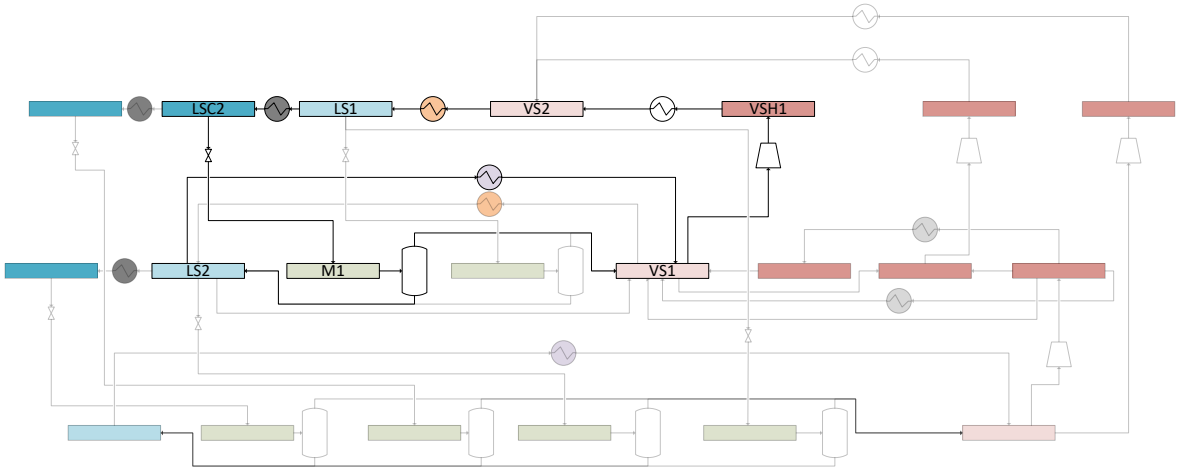

Figure 8. Example of basic refrigeration Cycle Scheme with Subcooling reproduced by the superstructure

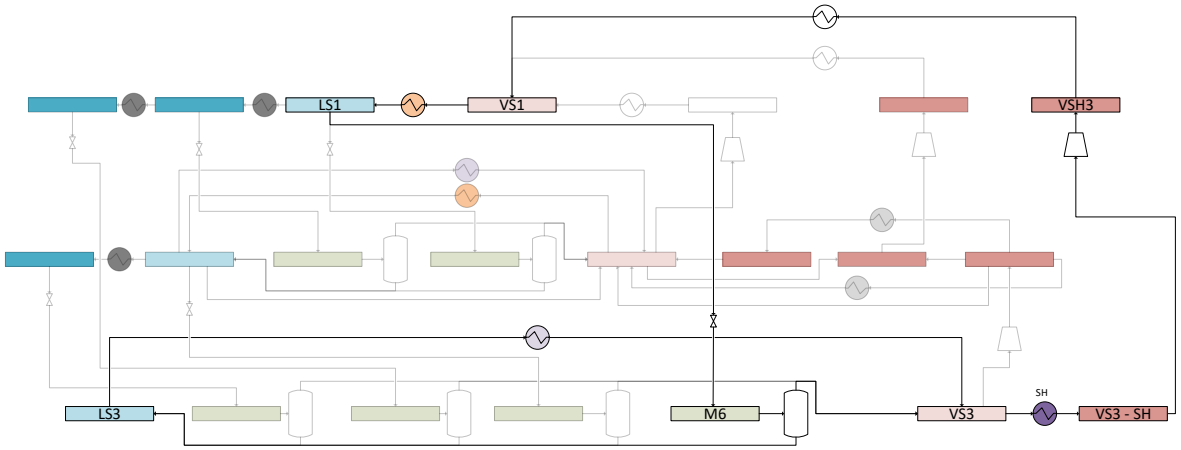

Figure 9. Example of basic refrigeration Cycle Scheme with superheating.

- Cascade Refrigeration Cycles. These designs are adopted when the temperature difference between heat sink and heat source (i.e., hot/cold process/utility streams to be heated/cooled) is so large that no working fluid is suitable for both temperature levels (e.g., too high triple point temperature, too low evaporation pressure, thermochemical decomposition limits, etc), or the heat integration with the heat source/sink stream would be considerably penalized by the shape of the saturation curve (e.g., too low critical temperature, too superheated, etc). In this case, two reverse cycles with different working fluids are combined in a cascade arrangement. A heat exchanger couples the evaporator of the higher temperature cycle with the condenser of the lower temperature cycle. In general, when dealing with processes with multiple hot/cold streams, other process/utility steams can receive or provide heat to these two exchangers increasing considerably the number of degrees of freedom. In terms of superstructures, a separated p-h superstructure must be considered for each refrigeration fluid used, as can be seen in Figure. In the proposed methodology the user has to fix the type of working fluid for each of the two cycles.

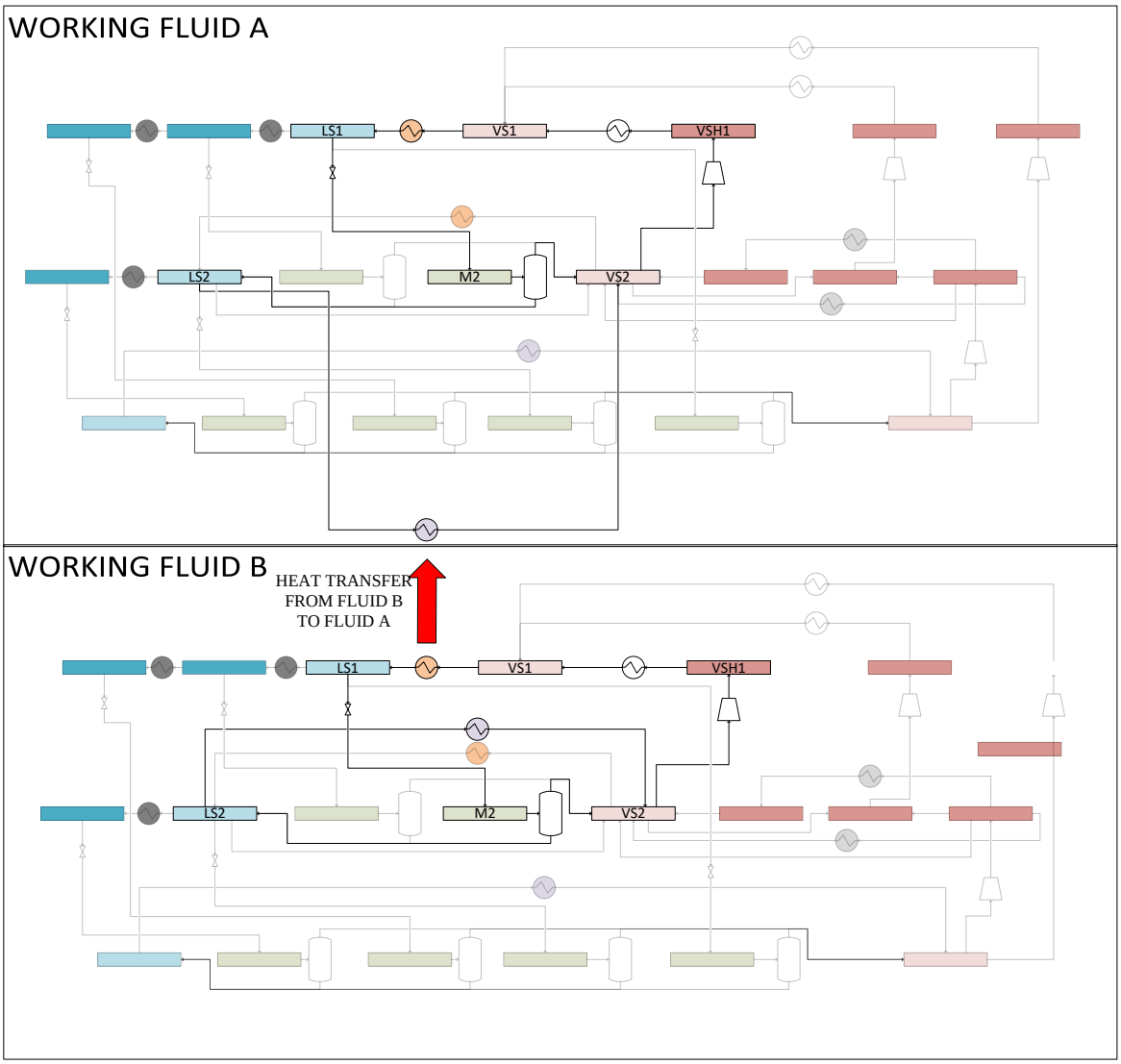

Figure 10. Example of cascade refrigeration cycle (2 basic cycles in cascade) which can be reproduced by the methodology.

Each header of the superstructure needs at this point fixed thermodynamic properties. They are calculated using a Matlab script calling REFPROP and then passed to GAMS before the optimization procedure starts. The main modelling equations for the cycle superstructure are the following:

- Mass balance equation for each header:

$$\sum_{u \in U \cap IN_{he}} \dot{m}_u = \sum_{u \in U \cap OUT_{he}} \dot{m}_u \quad \forall\, he \in HE \qquad \text{Eq. (3.1)}$$

- Energy balance equation for each header (note that at this point enthalpies are parameters, the only variables are, as in the mass balance, the mass flowrates):

$$\sum_{u \in U \cap IN_{he}} \dot{m}_u h_u = \sum_{u \in U \cap OUT_{he}} \dot{m}_u h_u \quad \forall\, he \in HE \qquad \text{Eq. (3.2)}$$

- Energy balance on heat-exchanging flows, where the variables are mass flowrate and exchanged heat, that will be used for heat exchanger areas and cost calculations:

$$\begin{gathered}
\left(T_{IN,i} - T_{OUT,i}\right)\dot{m}_i c_{P,i} = \sum_{k\in K}\sum_{j\in J} q_{ijk} \quad \forall i \in I \cap U, i \notin ISO \\
\left(T_{OUT,j} - T_{IN,j}\right)\dot{m}_j c_{P,j} = \sum_{k\in K}\sum_{i\in I} q_{ijk} \quad \forall j \in J \cap U, j \notin ISO \\
\dot{m}_i \lambda_i = \sum_{k\in K}\sum_{j\in J} q_{ijk} \quad \forall i \in I \cap U \cap ISO \\
\dot{m}_j \lambda_j = \sum_{k\in K}\sum_{i\in I} q_{ijk} \quad \forall j \in J \cap U \cap ISO
\end{gathered} \qquad \text{Eq. (3.3)}$$

It should be noted that the equations are different for isothermal and non-isothermal streams: in the first case the specific latent heat (condensation or evaporation) of an isothermal stream λ is used. In both cases two versions of the equation are used, one for hot streams I, the other for cold streams J.

- Objective function: it contains fixed costs C_f, heat exchangers cost, utility costs (cold and hot C_{CU} and C_{HU}) and electricity cost (with positive contribution to cost for compressors and negative for turbines). All the cost are discounted at a given interest rate by using the levelized Capital Carrying charge Rate and a multiplication factor.

$$\begin{aligned}
min\, TAC = CCR\, MF \Bigg(& \sum_{u\in U} C_{F,u} y_u + \sum_{i\in I}\sum_{j\in J}\sum_{k\in K} C_{F,ij} z_{ijk} \\
& + \sum_{u\in U, u\notin (I\cup J)} C_{S,u} S_{REF,u} \left(\frac{\dot{m}_u \Delta h_u}{S_{REF,u}}\right)^{\alpha_u} \\
& + \sum_{i\in I}\sum_{j\in J}\sum_{k\in K} F_{M,ij} F_{P,ij} C_{A,ij} A_{REF,ij} \left(\frac{A_{ijk}}{A_{REF,ij}}\right)^{\beta_{ij}} \Bigg) + \sum_{i\in I} C_{CU,i} q_{CU,i} \\
& + \sum_{j\in J} C_{HU\,j} q_{HU,j} - h_{EQ} p_{EL} \left(\sum_{u\in U\cap TURB} \dot{m}_u \Delta h_u - \sum_{r\in U\cap COMPR} \dot{m}_u \Delta h_u \right)
\end{aligned} \qquad \text{Eq. (3.4)}$$

Together with these equations, several others are used to model streams selection and particular needs: more details about the modelling equations of the cycle superstructure can be found in Appendix A.

3.2 Reverse Rankine cycle superstructure for optimization with variable p and T of headers

Considering also pressure and temperature of headers as decision variables allows performing three key simplifications on the above-described superstructure:

- For each pressure level just one subcooled header can be considered instead of a discretized sequence: in fact, if subcooling is selected the code will be able to optimize its temperature for the lamination at the selected pressure level.
- There is no longer need to perform a sensitivity analysis on the superheating degree at the outlet of the evaporators since the optimization will determine the optimal value. The lower bound of the interval is set to 1 K (safety value to avoid liquid droplets entering in the compressor).
- There is no need of guessing and fixing a priori the enthalpies (or temperatures) of header VSH5 resulting from the non-isothermal mixing of vapor streams at different temperatures.

The resulting superstructure in showed in Figure 11. It should be noted that, even if the structure can become simpler (especially with many pressure levels involved), the optimization becomes much more challenging due to the large number of variables and nonlinear relations between temperatures, pressures, enthalpies and entropies of the headers.

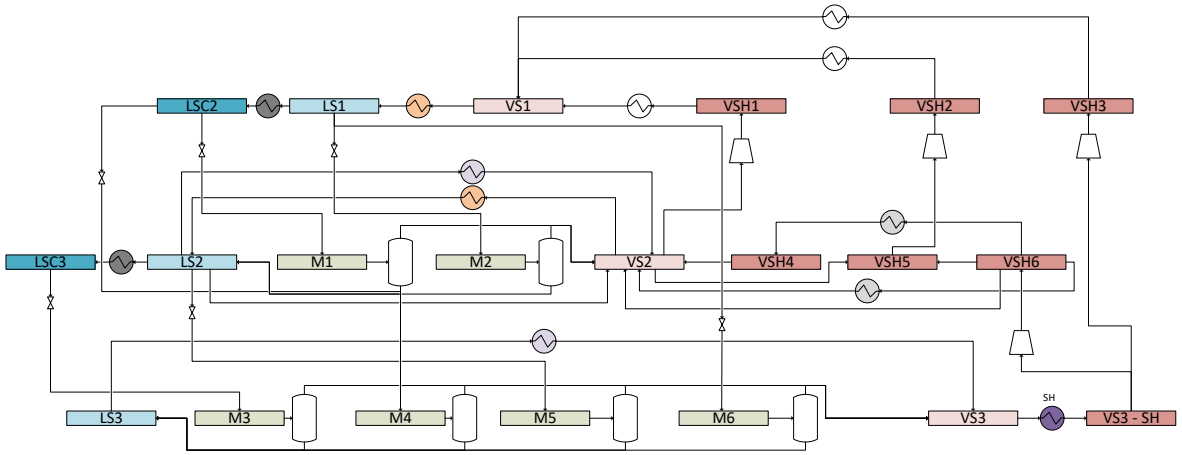

Figure 8. General Reverse Rankine Cycle Superstructure adopted for the optimization of pressures and temperatures of the headers.

In difference from the previous case, the thermodynamic properties of the headers are not fixed, so they cannot be computed before the optimization procedure.

The properties of the working fluid in each header are evaluated as functions of pressures and temperature by means of the Extrinsic Functions developed by Manassaldi et al. [24]. For example, from saturation temperatures and pressures (related using Antoine's equation), the functions compute the enthalpy and entropy values. Among the different available options, the Peng Robinson Equation of state was chosen for modelling the thermodynamic properties of the system. The iso-entropic efficiency definition was used to calculate properties at compressors outlet. The extrinsic functions are implemented in DLLs (Dynamic Link Libraries), and are available online at the official GAMS page as support material, together with a user's manual that explains the correct procedure to implement these functions in a script (Manassaldi et al. [25]). Comparison with REFPROP for the working fluids considered in the case studies (Propane, Ethane, Ammonia) indicates that the error

committed to the use of the Peng Robinson Equation of state in evaluating the enthalpies of the headers is lower than 1%, acceptable for the structural optimization purposes of this work.
The extrinsic functions are defined for single phase regions (liquid phase or vapor phase) and require as inputs pressure and temperature to calculate enthalpy, entropy and fugacity. The functions can handle a wide variety of pure fluids and mixtures (e.g., mixed refrigerants).
The overall formulation of the MINLP containing all the modelling equations can be found in Appendix B. The main groups of equations are reported below.

- All the equations detailed in the previous section for the model with fixed pressures and temperatures of headers (note that, in this modified formulation, all the temperatures and enthalpies become variables, thus increasing required equations, model dimension and complexity).
- Antoine's Equation: it is needed to relate saturation temperature and pressure of the condensation/evaporation levels.

$$p = exp\left(A - \frac{B}{tvar + C}\right) \qquad \text{Eq. (3.5)}$$

- Equations linking enthalpy and entropy to temperature and pressure: as stated before, the extrinsic functions developed by Manassaldi et al. [24] were used for this purpose. They come in two different forms, one for liquid phase calculation and one for vapor phase:

$$h_{he} = h_{liq}(T,p)\ \forall\ he \in HE$$
$$h_{he} = h_{vap}(T,p)\ \forall\ he \in HE \qquad \text{Eq. (3.6)}$$

$$s_{he} = s_{liq}(T,p)\ \forall\ he \in HE$$
$$s_{he} = s_{vap}(T,p)\ \forall\ he \in HE \qquad \text{Eq. (3.7)}$$

Due to their form, the application was differentiated depending on the phase of each header, for mixed ones no calculation needs to be made since they are obtained from iso-enthalpic valves, so their enthalpy is known.

- Valves outlet condition calculation:

$$h_{u,IN} = h_{u,OUT} \quad \forall\ u \in VALVES \qquad \text{Eq. (3.8)}$$

Eq. (3.8) is the energy balance of the valve (under assumption of steady flow, adiabatic transformation and comparable inlet/outlet kinetic energy) indicating that the enthalpy remains constant.

- Vapor-liquid separators:

$$\dot{m}_{in} = \dot{m}_{out,vap} + \dot{m}_{out,liq} \quad \forall\ he \in M \qquad \text{Eq. (3.9)}$$

$$\dot{m}_{in}h_{in} = \dot{m}_{out,vap}h_{out,vap} + \dot{m}_{out,liq}h_{out,liq} \quad \forall\ he \in M \qquad \text{Eq. (3.10)}$$

$$h_{u,IN} = h_{u,OUT} \quad \forall\ u \in SEP \qquad \text{Eq. (3.11}$$

Eq. (3.9) is the mass balance equation of the separator with $\dot{m}_{in}$denoting the inlet two-phase flow, $\dot{m}_{out,vap}$ the outlet saturated vapor flow, $\dot{m}_{out,liq}$ the outlet saturated liquid flow. Eq. (3.10) is the energy balance equation where h_{in} is the two-phase inlet enthalpy, $h_{out,liq}$ is the saturated liquid

enthalpy and $h_{out,vap}$ is the saturated vapor enthalpy. Eq. (3.11) is used to force the outlet enthaply of the two-phase headers to match the destinationation headers (i.e. to impose that the two flows that leave each two-phase headers are saturated liquid and saturated vapor, and their flowrates are determined by mass and energy balances).

- Compression outlet conditions calculations based on iso-entropic efficiency definition:

$$s_{in} = s_{out} \quad \text{Eq. (3.12)}$$

$$h_{out,iso} = h_{vap}(s_{out}, p_{out}) \quad \text{Eq. (3.13)}$$

$$h_{out} = h_{in} + \frac{h_{out,iso} - h_{in}}{\eta_{iso}} \quad \text{Eq. (3.14)}$$

Where s_{in} and s_{out} denotes the compressor inlet and outlet entropies, $h_{out,iso}$ is the isentropic outlet enthalpy and η_{iso} is the isentropic compressor efficiency.

3.3 HEN superstructure

Both versions of the optimization approach (i.e., fixed and variable pressure and temperature of the headers) adopt the well-known SYNHEAT superstructure proposed by Yee and Grossmann [21] to optimize the HEN synthesis. This structure, as seen in Figure 9, allows modelling both series and parallel heat exchangers by dividing the evaluation in stages and considering for each stage all the possible couplings. Following the successful approach of Martelli et al. [26] and Elsido et al. [19], the streams of the reverse Rankine cycle are included in the HEN in all the stages. Following the nomenclature proposed by Martelli et al. [26], all reverse Rankine cycle streams are handled as "HEN utility streams," while cooling water, cooling air and boilers (hot utility) are handled as "END utility streams" (they can be placed only in the hot or cold end stages of the HEN superstructure). Compared to classic approaches that handle the evaporator/condenser of the Rankine cycles as END utility (see, e.g., Yee and Grossmann, [21]), the approach proposed by Martelli et al. [26] and Elsido et al. [19] allows generating more efficient and cost effective HEN designs because of the more flexible heat integration options between cycle, utility and process streams. For a thorough analysis of the advantages of handling Rankine cycle and utility streams as "HEN utility streams", the reader is referred to Martelli et al. [26]. Since Rankine cycle streams are handled within the HEN superstructure model as process streams with variable mass flow rate, the optimization problem involves bilinear terms given by the products of stream mass flowrate and temperature at the inlet of each superstructure stage. Such bilinear terms are nonconvex and increase considerably the complexity of solving the Mixed Integer Non-Linear Programming model to global optimality, as described in Elsido et al. [19].

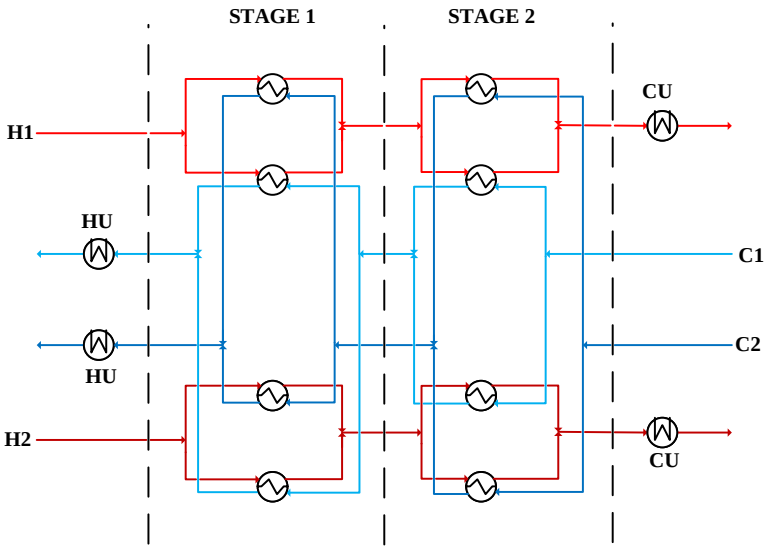

Figure 9. Scheme of the SYNHEAT structure for two hot streams, two cold streams and two temperature stages

As for the cycle superstructure equations, the modelling equations of the HEN superstructure are detailed in Appendix A. The most important are the following:

- Heat transfer direction:

$$q_{ijk} \geq 0 \quad \forall\, i \in I, j \in J, k \in K \qquad \text{Eq. (3.15)}$$

where k denotes the number of the stage, i and j are respectively the indexes for the hot and cold streams.

- Monotonic temperature variation:

$$t_{i,k} \geq t_{i,k+1} \quad \forall i \in I, i \notin ISO, k \in K$$

$$t_{j,k} \leq t_{j,k+1} \quad \forall \mathrm{j} \in \mathrm{J}, \mathrm{j} \notin ISO, k \in K$$

$$T_{OUT,i} \leq t_{i,NOK+1} \quad \forall i \in I, i \notin ISO \qquad \text{Eq. (3.16)}$$

$$T_{OUT,\mathrm{j}} \geq t_{j,NOK+1} \quad \forall \mathrm{j} \in \mathrm{J}, \mathrm{j} \notin ISO$$

- Energy balance for the non-isothermal streams at each stage of the superstructure. These terms are bilinear terms since both flowrate and temperature at any stage are variables. They are non-convex terms that increase complexity significantly.

$$\left(t_{ik} - t_{i,k+1}\right)\dot{m}_i c_{P,i} = \sum_{j \in J} q_{ijk} \quad \forall i \in I \cap U, i \notin ISO$$

$$\left(t_{j,k+1} - t_{jk}\right)\dot{m}_j c_{P,\mathrm{j}} = \sum_{j \in J} q_{ijk} \quad \forall \mathrm{j} \in \mathrm{J} \cap U, \mathrm{j} \notin ISO \qquad \text{Eq. (3.17)}$$

- Logical constraints, involving upper and lower bounds of variables and binary variables y and z to define the activation of streams and existence of heat exchangers.
  - Activation/deactivation of utility streams:

$$\dot{m}_u \leq y_u \dot{m}_{MAX,u} \quad \forall u \in U$$

$$y_u \dot{m}_{MIN,u} \leq \dot{m}_u \quad \forall u \in U \qquad \text{Eq. (3.18)}$$

- Heat exchangers existence:

$$q_{ijk} - \Omega_{MAX,ij} z_{ijk} \leq 0 \quad \forall i \in I, j \in J, k \in K \qquad \text{Eq. (3.19)}$$

- Heat exchangers areas:

$$A_{ijk} - A_{MAX,ij} z_{ijk} \leq 0 \quad \forall i \in I, j \in J, k \in K \qquad \text{Eq. (3.20)}$$

- Calculation of heat exchangers area: this term represents another important source of non-linearity, due to the multiplication of the exchange area and the Chen approximation [27] of the logarithmic mean temperature difference of heat exchange:

$$q_{ijk} \leq U_{ij} A_{ijk} \left(dt_{ijk} dt_{ijk+1} \frac{dt_{ijk} + dt_{ijk+1}}{2} \right)^{1/3} \quad \forall i \in I, j \in J, k \in K \qquad \text{Eq. (3.21)}$$

4. Optimization approach

4.1 Optimization approach for Fixed p and T of Headers

The optimization problem resulting from combining the superstructure of the Reverse Rankine cycle with fixed pressure and temperature of headers (Section 3.1) and HEN synthesis (section 3.3) gives rise to a nonconvex MINLP (Mixed Integer Non-Linear Program). It shares the same features (nonlinearities) and type of variables and constraints as the one derived by Elsido et al. [19] for power Rankine cycles (steam cycles and Organic Rankine cycles). More specifically, it features binary variables defining cycle components selection and heat exchangers activation, continuous variables for thermal power, areas, HEN *stage* temperatures, power of compressors, mass flow rates of Rankine cycle streams. The non-linearities are bilinear products in energy balances (mass flow rate of cycle streams times HEN stage temperatures, see Eq. (3.17)), heat exchanger areas calculation depending on the mean temperature difference (see Eq. (3.21)) and economy of scale in the capital cost of the equipment units (compressors and heat exchangers, see Eq. (3.4)). The overall model formulation can be found in Appendix A.

Since general purpose MINLP algorithms (such as BARON) cannot efficiently solve the MINLP to global optimality, Elsido et al. [19] proposed a bilevel decomposition algorithm very effective on this class of problems even on problem with tens of hot and cold streams. At the higher level, a linearized version of the problem (i.e., a Mixed Integer Linear Program, MILP) optimizes the integer variables (representing existence of streams and heat exchangers) and fixes them for the lower-level problem, a Non-Linear Program (NLP), which optimizes the continuous variables. The master problem MILP is obtained with the following linearization techniques applied to the original MINLP:

- McCormick relaxation [28] of bilinear terms in energy balances (products temperature-flowrate).

- Adaptive piecewise linearization of capital cost functions appearing in the objective function.
- Taylor's linearization of equation defining the heat exchanger areas (see details in Elsido et al. [19]).

After each master-lower iteration, binary solutions previously found by the MILP are excluded by adding integer cut constraints (so called "utility" and "HEN" cuts in Elsido et al. [19]). The master MILP is updated by linearizing the capital cost functions and HXs areas around the newly found solution, and a new iteration is performed. The algorithm proceeds by saving the best-found solution, and it stops when no improving solution is found for 20 consecutive iterations. In this version of the algorithm, the objective function value returned by the master MILP cannot be considered as a rigorous estimate of the lower bound of the solution. However, to determine the lower bound of the MINLP and check global optimality of the returned solution, a different linearization of the HX area relation can be adopted, as shown in Elsido et al. [19].

A good initial solution is found by a sequential approach using the Energy Targeting Methodology of Marechal and Kalitventzeff [8] to find the cycle structure and mass flow rates of working fluid in each cycle branch, which maximize efficiency considering the cycle thermally integrated with the process heat cascade. The energy targeting model is formulated as an MILP and it can be rapidly solved due to the very limited number of variables (the combinatorial complexity of the HEN solution is avoided and replaced by the heat cascade). Then, for fixed cycle structure and mass flow rates, the Minimum Number of Units problem is solved as an MILP using the Yee and Grossmann [21] superstructure. The HEN structure found with the Minimum Number of Units problem is transferred to the NLP subproblem to minimize the total annual cost by varying all the real variables while keeping fixed all the binary (i.e., structural) variables. At this point, the bilevel optimization algorithm begins (alternating the solution of the master linearized problem and the NLP subproblem).

As for the solvers, IBM ILOG CPLEX version 12.8 [29] is used for the initialization procedure and for the master MILP problem, while BARON version 17.10.16 [30] is used to solve the NLP subproblem. BARON is a solver for NLP and MINLP problems, implementing deterministic global algorithms guaranteed to find the global optimum. The basic algorithm is a spatial Branch and Bound algorithm, combined with several other techniques.

Table 1 shows the advantage of using the bilevel decomposition algorithm compared to solving the overall monolithic MINLP related to case studies 1 and 2 (see Section 5.1) using BARON as MINLP solver with a maximum computational time set to 20000 seconds. The results obtained with the bilevel decomposition approach on case study 1 are better than the ones found by BARON and the required computational time is considerably shorter. In case study 2, BARON cannot find a feasible solution for the problem, while the bilevel decomposition algorithm finds a feasible solution in the first iteration and an optimized solution in 14880 seconds. It is worth noting that allowing the optimization of the headers pressures and temperatures further worsens the performance of MINLP solvers making it necessary to decompose the problem (see Section 4.1).

Table 1. Comparison between the performance of the bilevel decomposition algorithm and BARON in solving the MINLP problem of case studies 1 and 2 with fixed pressures and temperatures of headers.

k€/yr	**Propane**	**R134a**	**Case Study 2**
Overall MINLP	5032,05	5007,24	no solution found
Lower Bound	4253,02	4506,86	no solution found
Bilevel Dec	5024,94	4720,97	113,95

4.1. Variable p and T of Headers Optimization

To tackle the MINLP problem with variable pressures and temperatures of the cycle headers, the bilevel decomposition algorithm has been adapted as discussed in this section. In particular, it was decided to keep the same master MILP problem as the original bilevel decomposition, and modify only the NLP subproblem by adding pressure, temperature and enthalpy of headers as variables. This modification leads to having additional nonlinear and nonconvex terms in the NLP problem, namely the products between mass flow rates and enthalpies in energy balances and the equations linking temperature and enthalpy (Eq. (3.2) and Eq. (3.6)). In the master problem, the temperatures, pressures and enthalpies of headers remain fixed (as parameters, not optimization variables), and their values are updated at each iteration with the values found by the NLP subproblem. It was decided to keep the header conditions as parameters in the master problem to keep it linear and not increase its complexity (since solving it is already challenging for problem with many hot and cold streams). Figure 10 shows the steps of the solution procedure, indicating with colours the steps differentiating variable-headers optimization from fixed-headers optimization.

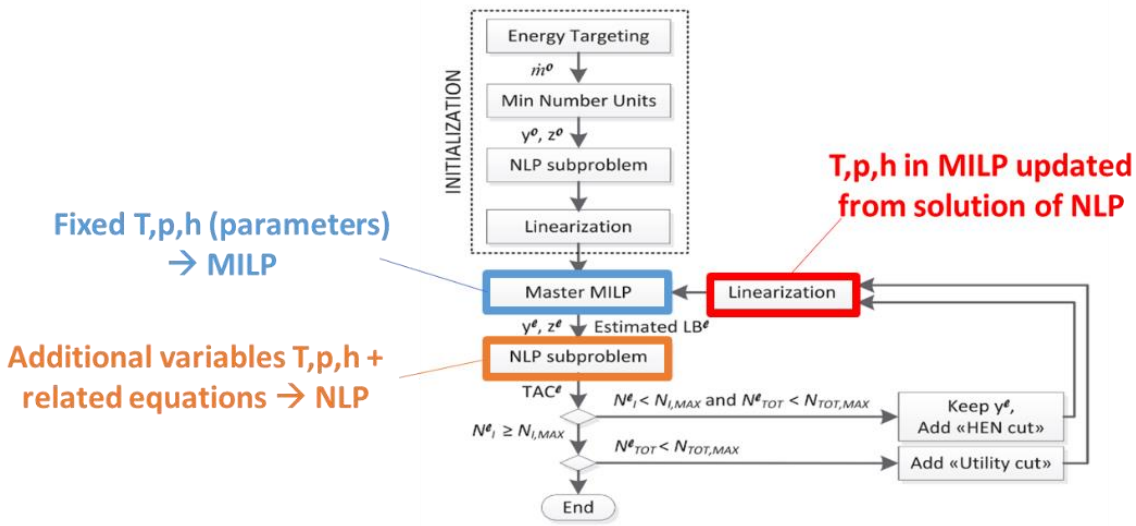

Figure 10. Block-flow diagram of the bilevel decomposition algorithm proposed to solve the MINLP problem with variable pressures and temperatures of cycle headers.

As for the NLP subproblem solution, the use of extrinsic functions affect the solver choice: due to the unavailability of the explicit algebraic expressions of the constraints related to the thermodynamic properties, the global solver BARON cannot be used for the NLP subproblem (because BARON needs the algebraic expression of all constraints in order to find the most suitable convexification and lower bound of the problem). As a replacement, MSNLP (Multi Start Non-Linear Programming) [31]

is chosen. Unlike BARON (which uses a rigorous spatial branch-and-bound strategy with global convergence guarantees), it is a local solver where the limitation of finding a local minimum is mitigated by considering multiple starting points. The multistart routine generates 1000 random starting points which are passed to CONOPT [32], a well-known local solver using a Generalized Reduced Gradient as optimization algorithm. Extended information about this algorithm can be found in Drud [32], [33].

5. Case Studies

The proposed method has been applied to four literature test cases selected according to the following criteria:

- Considering different refrigeration fluids, including ammonia, propane, ethane and R134a.
- Featuring different possible architectures in terms of number of pressure levels (up to seven possible levels) and cycle configuration.
- Featuring an increasing number of process streams to be thermally integrated with the refrigeration cycle and the HEN.
- One of the case studies (case study 4) also features a cascade refrigeration cycle configuration.

The key features of the four case studies are detailed below while the stream data (process stream temperatures and heat duty) and cost-related data are reported in Table 2.

Table 2. Data for the four case studies: flowrates and inlet/outlet temperatures of process streams

Flowrate (kW/K)	**Case Study 1**	**Case Study 2**	**Case Study 3**	**Case Study 4**
Hot 1	96.1	10	10	100
Hot 2	-	-	10	-
Cold 1	-	40	15	-
Cold 2	-	-	10	-
Tin - Tout (K)	**Case Study 1**	**Case Study 2**	**Case Study 3**	**Case Study 4**
Hot 1	313-220	440-250	360-320	190-190
Hot 2	-	-	320-250	-
Cold 1	-	270-300	260-310	-
Cold 2	-	-	300-360	-
	Case Study 1	**Case Study 2**	**Case Study 3**	**Case Study 4**
n. levels in superstructure	4	6	7	6/6*
HX data				
$UF*C_{ref}$ ($)	1050	13750	13750	13750
S_{ref} (m^2)	10000	37,16	37,16	37,16
f	0,75	0,65	0,65	0,65
Compressors data				
C_{ref} ($)	6300	-	-	-
S_{ref} (kW)	10000	-	-	-
f	0,67	-	-	-

Cf ($/yr)	-	2824,8	2824,8	2824,8
Cv ($/kWyr)	-	831,67	831,67	831,67
Other data				
Electricity Cost ($/kWyr)	560	608,33	608,33	608,33
CW cost ($/kWyr)	20	31,94	31,94	31,94
CW temperature (K)	288-298	300-305	300-305	300-305
Steam Cost ($/kWyr)	-	50,91	50,91	-
Steam temperature (K)	-	440	440	-
Equivalent hours	7000	7000	7000	7000
CCR	0,3	0,3	0,3	0,3

* 6 levels for each refrigerant

5.1. Case Study 1: Single-refrigerant CO_2 liquefaction cycle

Case study 1 is a refrigeration cycle for CO_2 liquefaction studied by Alabdulkarem et al. [2]. It represents an example of a typical low-temperature application of refrigeration cycles. The cycle as to cool a stream of CO_2 to 220 K, and the heat sink of the refrigeration cycle is cooling water (CW). For this case study propane is considered as the working fluid.

Since ref. Alabdulkarem et al. [2] does not provide capital cost correlations for compressors, heat exchangers (necessary for the optimization of the TAC), these missing capital cost correlations are assumed to be according to the well-known economy of scale power law (Eq. (5.1)).

$$C = C_{ref}\left(\frac{S}{S_{ref}}\right)^{f} \qquad \text{Eq. (5.1)}$$

In Eq. (5.1) C represent the capital cost, C_{ref} the cost at the reference size S_{ref}, and S the unit size (power for compressors and heat transfer area for HXs) and f is the the scaling factor. Coefficients S_{ref}, C_{ref} and f are taken from Xu et al. (2014)[34] for HXs and Elsido et al. [19] for compressors.

The refrigeration cycle configuration found by Alabdulkarem et al. [2] is represented in Figure 12 and it involves one level of condensation and two levels of evaporation. The peculiarity of the configuration is that the lamination starts from the condensation pressure for both the levels of evaporation. The same cycle solution has been re-built using the superstructure and stream property calculation described in Sections 2 and 3 in order to check the accuracy of our model (validation) and compute the COP and economic performance using our basis. The COP of such solution is 1.17, with a total annual cost of 7103,54 k$/year. It is worth noting that the values of COP is very similar (about 3.5% error) to the one obtained in Alabdulkarem et al. [2] confirming the accuracy of our cycle model. As far as the cost is concerned, the authors of the case study performed an optimization based on the COP and no cost is calculated, for this reason no comparison can be made in terms of cost for this case study.

As far as the optimization is concerned, a superstructure with up to 4 pressure levels has been considered. Compared to the reference study Alabdulkarem et al. [2], an intermediate pressure levels of evaporation of evaporation/condensation is added at the first-guess temperature of 1°C. In the optimization with fixed pressure and temperature of cycle headers, the pressures/temperatures of the other three levels is set in agreement with the reference study. Instead, in the optimization with variable pressure and temperature of headers, all four pressure levels and superheating/subcooling temperatures are optimized.

5.2. Case Study 2: Example *E1* published by Shelton and Grossmann [6]

Case study 2 is taken from ref. Shelton and Grossmann [6] and it features a hot process stream to be cooled from 440 to 250 °C, and a cold process stream to be heated up from 270 to 330 °C. The two streams can be thermally integrated to save some refrigeration power. If necessary, steam at 440 °C and cooling water at 300-305°C can be used as utility flows (here modelled as hot and cold end utility respectively). Of course, the heat integration between hot and cold streams of process, utility and refrigeration cycles yields a large variety of possible HEN configurations. The refrigeration cycle uses ammonia (NH_3) as working fluid and the superstructure considered in Shelton and Grossmann [6] considers up to six pressure levels, each one equipped with a direct contact heat exchanger/separator and the possibility of intermediate hot and cold loads.

The same cost-related assumptions reported in reference article are kept here for comparison. In particular, for the compressors a linear expression was used for the total annualized cost (sum of annualized capital cost and annual operating cost):

$$Cost = C_f + C_v * Power \qquad \text{Eq. (5.2)}$$

where C_f represents fixed costs and C_v variable costs (reported in Table 2).

As for the heat exchangers, the same power law correlation reported in Eq. (5.1) was selected by authors of Shelton and Grossmann [6], updated using Guthrie's factor and the coefficients are reported in Table 2.

The optimized refrigeration cycle and HEN obtained by Shelton and Grossmann [6] are represented in Figure 13. The COP is 5.73, the capital cost is 87.949 k$/year, the operating cost is 54.283 k$/year and the TAC is 142.232 k$/year. It is worth noting that the value of TAC is very similar (about 4.5% error) to those reported in Shelton and Grossmann [6] of 142.232 k$/year confirming the accuracy of our model.

For the optimization, a superstructure with up to 6 pressure levels is considered in agreement with that considered by the reference work). In the optimization with fixed pressure and temperature of cycle headers, the pressures/temperatures of the six levels is set equal to those considered by reference study. Instead, in the optimization with variable pressure and temperature of headers, all six pressure levels and subcooling/superheating temperatures are optimized.

5.3. Case Study 3: Example *E2* published by Shelton and Grossmann [6]

Case Study 3 is example E2 by Shelton and Grossmann [6], and it consists in a more complex version of previous case 2 featuring more hot and cold process streams (i.e., two hot and two cold streams). It represents a more challenging problem, used as benchmark also in different more recent studies (e.g., [1]). The refrigeration cycle superstructure considers ammonia as working fluid and up seven pressure levels.

The optimized refrigeration cycle and HEN obtained by Shelton and Grossmann [6] are represented in Figure 14. The COP is 7.00, the capital cost is 94.098 k$/year, the operating cost is 39.994 k$/year and the TAC is 134.092 k$/year. It is worth noting that the value of TAC is very similar (about 4.3% error) to the one reported in Shelton and Grossmann [6] of 128.540 k$/year, confirming the accuracy of our cycle model.

A superstructure with up to 7 pressure levels is considered in agreement with that considered by the reference work. The superstructure is shown in Figure 11. In the optimization with fixed pressure and temperature of cycle headers, the pressures/temperatures of the seven levels is set equal to those considered by reference study. Instead, in the optimization with variable pressure and temperature of headers, all pressure levels and subcooling/superheating temperatures are numerically optimized.

5.4. Case Study 4: Example *1* published by Vaidyaraman and Maranas [17]

Case Study 4: *Example n. 1* by Vaidyaraman and Maranas [17] is a propane-ethane cascade refrigeration cycle with only one hot process stream with a 100 kW cooling duty at 190 K. It was chosen to evaluate the capability of the model to deal with cascade cycles and, hence, a large number of alternatives and variables. In this case study the only available cold sink is cooling water, available between 288 K and 298 K.

As far as the cost assumptions are concerned, the authors referred to Shelton and Grossmann [6], while some strong assumptions are made regarding other points:

- Minimum compression cost is used as objective function, ignoring heat exchangers and utilities
- Ideal gas is assumed by the authors of the case study

Moreover, different solutions are proposed, the comparison is made with respect to the most performing one. Since the ideal gas assumption (especially at such low temperatures) was considered too strong, the performance and cost associated to the structured proposed by Vaidyaraman and Maranas [17] were re-calculated keeping the same temperature and pressure of the levels.

The optimized structure by Vaidyaraman and Maranas [17] is composed of a cascade cycle with 6 levels on the high pressure (propane) cycle and 4 levels on the low pressure (ethane) cycle, as reported in Figure 15. The refrigerant switch happens between 232 K and 236 K by coupling the lower cycle condenser with the upper cycle evaporator. This results in a COP of 1.297, an investment cost of of 99.586 k$/year, an operational cost of 52.552 k$/year and a TAC of 152.138 k$/year. The results are different from the ones obtained by the authors of the case study, mainly due to the ideal gas hypothesis that was removed.

Two superstructures with up to 6 pressure levels are considered. Compared to the original reference, two more pressure levels are considered for the low temperature cycle to give more flexibility. In the optimization with fixed pressure and temperature of cycle headers, the pressures/temperatures of the seven levels is set equal to those considered by reference study, and the additional temperature levels of the low temperature cycle are set to 258 K, 273 K. Instead, in the optimization with variable pressure and temperature of headers, all pressure levels and subcooling/superheating temperatures of both cycles are numerically optimized with a considerable increase in complexity.

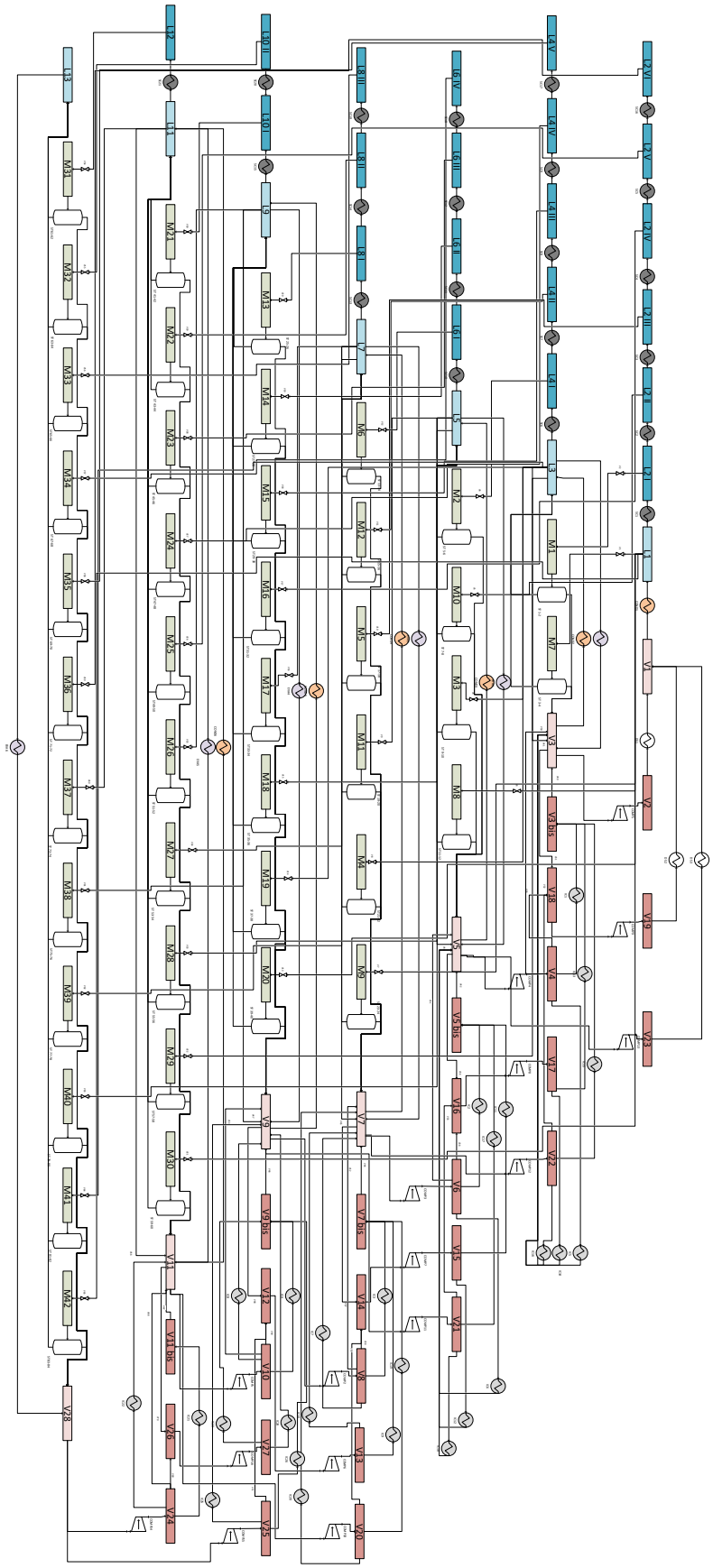

Figure 11. Superstructure with seven levels of pressure

6. Results

For each case study, the iterative procedure of the bilevel algorithm has been executed considering as stopping criterion if the best solution found does not improve after 20 consecutive iterations. * Includes also the initialization with fixed p and T of headers shows the iterations at which the algorithm found the optimal solution, and the total computational time to reach the stopping criterion. The computational times associated to the variable optimization include also the time required by the fixed optimization to find the best possible starting point.

Table 3. Problem sizes, iteration at which optimal solution is reached and corresponding time for convergence

	Case Study 1	**Case Study 2**	**Case Study 3**	**Case Study 4**
Real variables	16 000	39 000	87 000	55 000
Binary variables	6 000	12 000	29 000	11 000
Constraints	25 000	58 000	129 000	88 000
Initialization (Fixed p and T of Headers): iteration # optimum found	69	33	28	25
Initialization (Fixed p and T of Headers): total iterations	89	53	48	45
Initialization (Fixed p and T of Headers): computational time (seconds)	2968	14880	17100	1758
Variable p and T of Headers: iteration # optimum found	80	60	51	29
Variable p and T of Headers: total iterations	100	80	71	49
Variable p and T of Headers: computational time (seconds) *	3738	26160	33547	2649

* Includes also the initialization with fixed p and T of headers

It is clear from the results that the required time for convergence depend mainly on heat integration possibilities and superstructure complexity for the refrigeration cycle. Case study 1 has a simple structure and only one process stream. Even if the best solution is found after many iterations with fixed p and T of headers, the required time for iteration is lower, as can be seen from the overall convergence time. Some more iterations are needed in the variable case, but they are even faster. This is due to the fact that the fixed p and T solution provides a very good starting point for the variable step, that can proceed faster. Case studies 2 and 3 are similar: complexity grows and also heat integration possibilities, leading to longer time requirements for convergence. In particular, case study 3 has the longest single-iteration time due to the combination of complexity and heat integration. In case study 4 the superstructure is very complex (two times the structure of case study 2), but heat integration possibilities are very limited as previously stated, leading to a solution converging in a number of iterations in the order of magnitude of case 2 and 3. Single-iteration time, on the other hand, is shorter due to lower heat integration possibilities offered by a single process stream at a very low temperature (190 K).

The results of the optimization are reported in Table 5. For all case studies, improvements in terms of performance (measured as TAC reduction) are found with the fixed p and T of headers optimization

approach. The optimization with variable pressures and temperatures of the headers further improve the performance.

The reported value is the value found by forcing the method proposed in this work to replicate the same structure proposed in the case study. This is done to validate the appropriateness of the assumptions made. The error with respect to the reference cost was below 5% in case studies 2 and 3 (in case study 1 no cost was given while in case study 4 the perferct gas asssumpion was removed, so the value changed).

Table 4. Performance results of the four case studies.

	Case Study 1	**Case Study 2**	**Case Study 3**	**Case Study 4**
Reference TAC_{REF} (k€/yr)	7103,5	142,2	134,1	152,1
Fixed p and T of headers TAC_F (k€/yr)	5024,9	114,0	97,6	151,3
Improvement: $(TAC_F\text{-}TAC_{REF})/TAC_{REF}$	29,3%	19,9%	27,2%	0,6%
Variable p and T of headers TAC_V (k€/yr)	4316,1	107,6	84,6	147,4
Improvement: $(TAC_V\text{-}TAC_{REF})/TAC_{REF}$	39,2%	24,3%	36,9%	3,1%
Reference COP_{REF}	1,17	5,73	4,09	1,30
Fixed p and T of headers COP_F	1,77	7,00	5,40	1,31
Variable p and T of headers COP_V	2,20	9,59	8,65	1,40

As far as the energy performance of the cycles are concerned, the COP values of the different case studies are reported in Table 4. The large values for case study 2 and 3 are due to the combination of the iso-entropic compression assumption (kept in this study for comparison reasons with the benchmark case), and of the heat integration allowed by the presence of cold process streams at low temperature in some other cases. In fact, being COP calculated as the ratio between the heat removed from the hot process streams and the compression power required for the task, the availability of a cold process streams greatly reduces the compression need by providing a lower temperature heat sink to be coupled with the condenser.

$$COP = \frac{Q_{HOT}}{P_{COMP}} \qquad \text{Eq. (6.1)}$$

where Q_{HOT} represents only the portion of heat subtracted from the hot stream by the refrigeration fluid in the evaporators, excluding the portion of heat directly exchanged with the cold streams (when present), which does not influence the cycle's efficiency and P_{COMP} is the overall compression power.

In this way, the condensation temperature is reduced, in turn reducing the compression requirement for reaching that temperature. In general, in all cases, the proposed methodology finds refrigeration cycle designs with higher COP compared to the reference case.

The case-dependent percentage improvement varies with the case study due to different approach adopted in the reference publication and the peculiarities of the case studies. In Case Study 1, for example, the reference solution was obtained with an approach not capable of optimizing the cycle structure. The results show how adopting synthesis methods (i.e., able to optimize also the structure of the cycle) leads to considerable improvements. Case Study 2 and 3, featuring several process streams to be heat integrated with the cycle, show how the proposed method performs better than

literature approaches because of the more rigorous optimization of the efficiency-area trade-off. It is worth noting that the same test case 3 is used as benchmark in Wallerand et al. [1] which found a solution with just 5,1% lower TAC (as a comparison, this work finds a solution with a TAC reduction of 36.9% due to the more systematic optimization of the HEN). For case study 4, the relative improvement is smaller compared to other cases because the reference cycle was well optimized and, due to the limited number of process streams, the heat integration problem features a limited number of possible HEN arrangements. However, the results still show that the approach is able to optimize the design of very complex cascade cycles obtaining improvements compared to ad-hoc approaches. Table 5 reports the cost comparison between solutions found in this work and the ones reported in previous work. The Reference column refers to the optimized structure found in literature.

Table 5. Costs of solutions found in the 4 case studies

		k€/yr	
Case Study 1	**Reference Cost** - Alabdulkarem et al. [2]	**This Work: Fixed p and T of headers**	**This Work: Variable p and T of headers**
HX	555,59	336,26	497,07
COMP	1945,52	1577,79	1282,73
ELECTRICITY	4271,11	2831,00	2276,24
CW	331,31	279,89	260,06
TOT	7103,54	5024,94	4316,11
Case Study 2	**Reference Cost** – Shelton and Grossmann [6]	**Fixed p and T of headers**	**Variable p and T of headers**
HX	30,814	37,722	40,832
COMP	57,135	33,799	27,011
ELECTRICITY	31,461	18,524	15,625
STEAM	22,822	23,905	24,147
TOT	142,232	113,950	107,615
Case Study 3	**Reference Cost** - Shelton and Grossmann [6]	**Fixed p and T of headers**	**Variable p and T of headers**
HX	32,000	47,140	43,673
COMP	56,980	26,021	20,291
ELECTRICITY	29,280	12,835	8,643
STEAM	10,280	11,653	12,004
TOT	128,540	97,649	84,611
Case Study 4	**Reference Cost** - Vaidyaraman and Maranas [17]	**Fixed p and T of headers**	**Variable p and T of headers**
HX	12,87	13,06	22,09
COMP	86,71	86,12	81,95
ELECTRICITY	46,90	46,47	39,96
CW	5,66	5,63	3,43
TOT	152,14	151,28	147,42

In Case study 1 the reference solution is considers a defined limited structure, optimizing only its temperatures and pressures with limited heat integration possibilities (only one process stream is available). In the optimized solution found in the present work, a pressure level is added as seen in Figure 15.

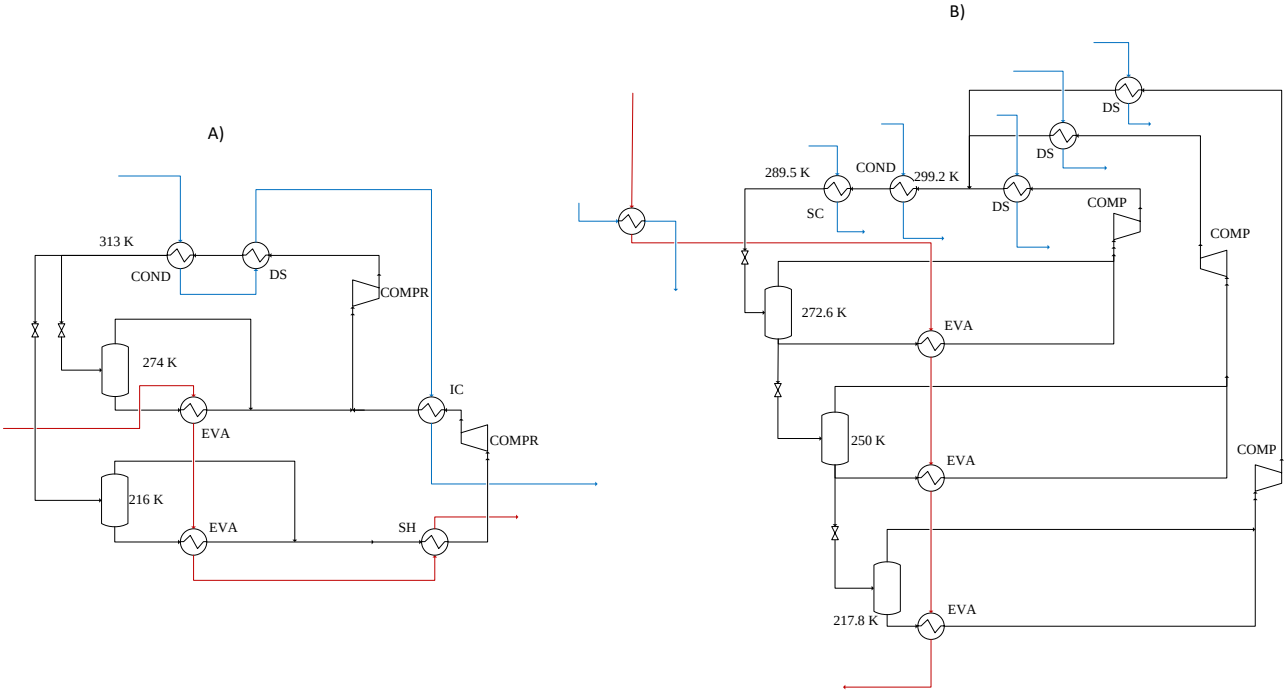

Figure 12. Starting (A) and optimal (B) structures of case study 1

On the other hand, a clear trend of progressive simplification of the cycle configuration is observed when going from the reference solution to the optimized one when significant heat integration options are available (Case studies 2 and 3, as can be seen in Figure 13 and Figure 14). Since the proposed methodology can consider the efficiency-cost trade-off rigorously, its trend is to reduce the number of pressure levels, avoiding to select when possible the higher pressure levels. This leads to a drop in required compression power, thus reducing also the capital costs of compressors and the operating cost due to the purchase of electricity.

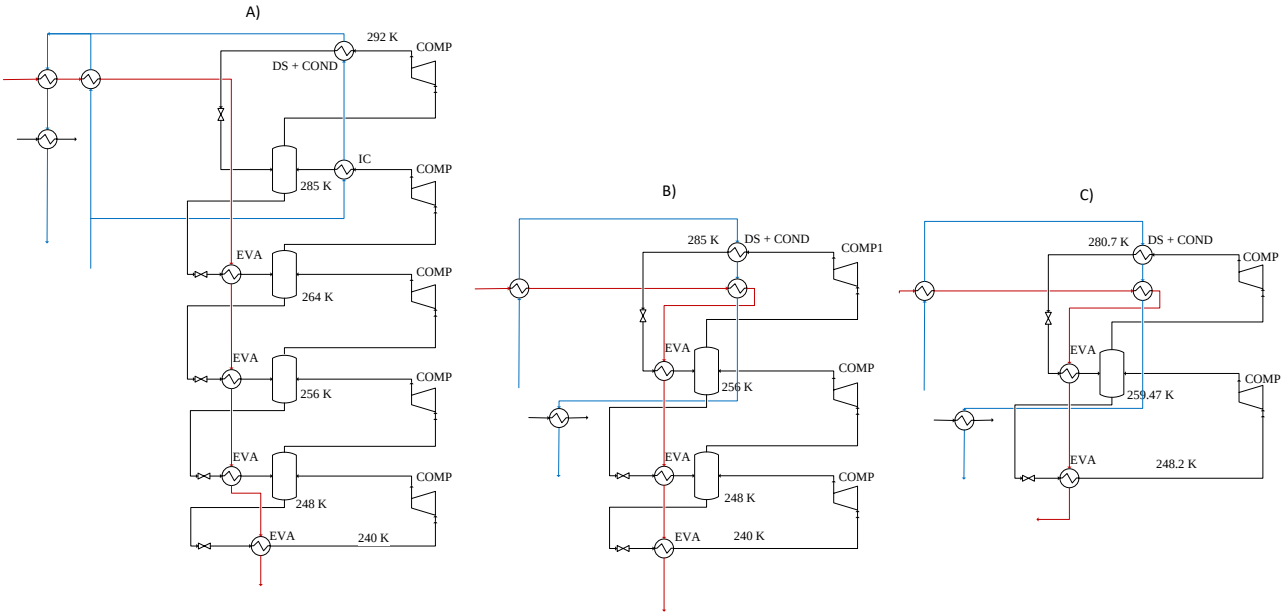

Figure 13. Scheme of Case study 2 evolution. From left to right: A) Solution proposed by Shelton and Grossmann [6], B) Fixed p and T of headers, C) Variable p and T of headers

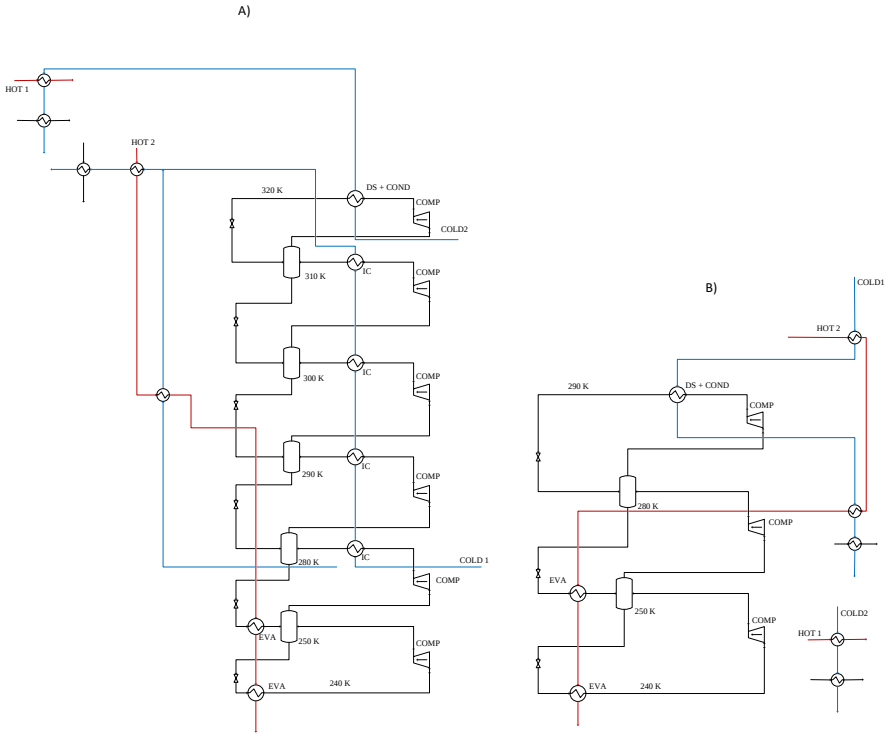

Figure 14. Starting (A) and optimal (B) structures of case study 3

In case study 4, the main changes from the solution proposed in literature are the addition of subcooling at the highest-pressure level and the direct contact cooler solution, which was chosen in place of the vapour mixing intercooler.

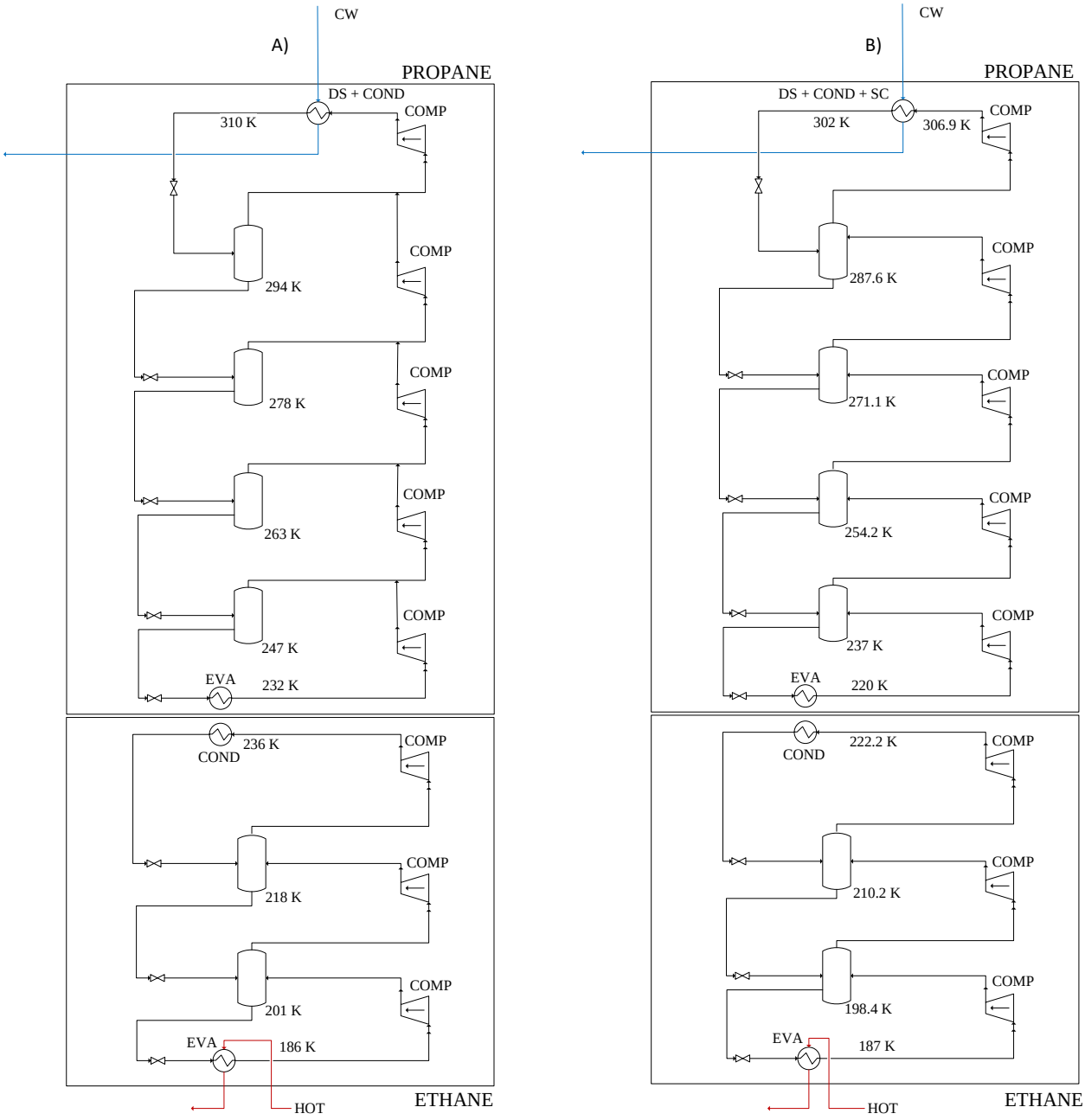

Figure 15. Starting (A) and optimal (B) structures of case study 4

Removing higher pressure levels has a positive effect on compression cost and COP, but decreses temperature difference across the highest level condenser. This leads to a higher area required for heat exchange, thus increasing the cost share of heat exchangers (see Table 5). This is particularly evident in case studies 2 and 3, where the structure undergoes the simplification process seen above, but the same behvior can be partially seen also in the other case studies.

7. Conclusions

In this work a method for the simultaneous optimization of refrigeration cycles and HEN has been developed. This method can select the best possible refrigeration cycle configuration and HEN

749 configuration, considering all the possible integration options between cycle and process streams as
750 well as the rigorous trade-off between efficiency and capital cost.
751 To the best of the authors' knowledge, no other method in literature achieves this level of generality,
752 combining the optimization of a very general compression refrigeration cycle superstructure
753 (containing all the main technological possibilities like sub-cooling, super-heating and different
754 intercooling options) with the optimization of HEN (both in terms of structure and temperature
755 differences) and thermodynamic properties (temperatures and pressures of all the selected levels).
756 The resulting model is a very challenging nonconvex MINLP problem, whose solution has been
757 addressed by adapting a bilevel decomposition approach based on advanced MINLP linearization
758 techniques, featuring up to 7 levels of pressure, 150 headers and 250 components (leading to models
759 with a size of 87,000 real variables, 29,000 binary variables and 129,000 equations).
760 The results of the case studies show that the developed model always provided optimal solutions
761 characterised by lower TAC and higher COP values compared to the benchmark solutions found in
762 previous works. It can be noticed from the analysis of the results that the performance improvement
763 is mainly proportional to heat integration possibility and the methodology can also optimize very
764 complex cascade cycles.
765 Future development of the presented method will focus on the application of the proposed method to
766 power cycles and multiperiod problems, where different operating conditions are considered.

Appendix A: Model formulation with fixed p and T of headers

Indices:

i = hot stream

j = cold stream

k = temperature stage

u = component of the p-h superstructure

he = header in the p-h superstructure

HU = hot "end utility"

CU = cold "end utility"

Sets:

I = set of hot streams i in the HEN (process stream or utility stream)

J = set of cold streams j in the HEN (process stream or utility stream)

P = set of hot process streams in the HEN

U = set of components of the p-h superstructure, e.g., compressor, economizer, evaporator, condenser, etc.

K = set of temperature stages

HE = set of headers in the p-h superstructure

ISO = set of process or "HEN utility" streams that are isothermal

SS = set of streams that cannot be split into branches (i.e., with "no stream splitting" constraint)

FM = set of couples of streams for which the match is forbidden

RM = set of couples of streams for which the match is restricted, i.e., a maximum amount can be exchanged

RQ = set of couples of streams for which the match is required, i.e., a minimum amount must be exchanged

IN_{he} = set of superstructure streams that enter header he

OUT_{he} = set of superstructure streams that exit header he

$TURB$ = set of turbines (with net power output), subset of components in the p-h superstructure

$PUMP$ = set of pumps (with net power input), subset of components in the p-h superstructure

$COMPR$ = set of compressors (with net power input), subset of components in the p-h superstructure

Parameters:

NOK = total number of stages

T_{IN} = inlet temperature of a stream

T_{OUT} = outlet temperature of a stream

F = flow rate of a process stream

c_P = specific heat capacity of a non-isothermal stream

λ = specific latent heat (condensation or evaporation) of an isothermal stream (in set ISO)

h = specific enthalpy of a header

h_{IN} = specific inlet enthalpy of a superstructure stream

h_{OUT} = specific outlet enthalpy of a superstructure stream

U_{ij} = overall heat transfer coefficient between hot stream i and cold stream j

Ω_{ij} = upper bound for heat exchange between hot stream i and cold stream j

$\Delta T_{MAX,ij}$ = upper bound for temperature difference between hot stream i and cold stream j

$\dot{Q}_{MAX,ij}$ = maximum heat that can be exchanged by streams $(i,j) \in RM$
$\dot{Q}_{MIN,ij}$ = minimum heat that can be exchanged by streams $(i,j) \in RQ$
$\dot{m}_{MAX,u}$ = maximum mass flow rate of a "HEN utility" stream u
$\dot{m}_{MIN,u}$ = minimum mass flow rate of a "HEN utility" stream u, if activated
$\dot{m}_u$ = mass flow rate of a "HEN utility" stream u, if activated
$A_{MAX,ij}$ = maximum area of a heat exchanger between hot stream i and cold stream j
$C_{F,ij}$ = fixed cost of activation for a match between hot stream i and cold stream j
$C_{A,ij}$ = specific area cost coefficient for a match between hot stream i and cold stream j, referred to area $A_{REF,ij}$
$A_{REF,ij}$ = reference area for the cost of a heat exchanger between hot stream i and cold stream j
β_{ij} = exponent for area cost for a match between hot stream i and cold stream j
$F_{M,ij}$ = material factor (i.e., the ratio between the specific area cost of the material and that of carbon steel) for a match between hot stream i and cold stream j
$F_{P,ij}$ = pressure factor (depending on the maximum pressure among the two fluids) for a match between hot stream i and cold stream j
$C_{F,ij}$ = fixed cost of activation for a component r of the p-h superstructure
$C_{S,u}$ = specific investment cost coefficient for a component u of the p-h superstructure (i.e., turbine, pump, compressor, etc.), referred to size $S_{REF,u}$
$S_{REF,u}$ = reference size for the cost of a component u of the p-h superstructure
Δh_u = specific enthalpy drops/increase (specific work) of turbines, pumps and compressors of the cycle superstructure
$C_{CU,i}$ = unit cost for cold "end utility" matched with hot stream i
$C_{HU,j}$ = unit cost for hot "end utility" matched with cold stream j
α_u = exponent for cost for component u of the p-h superstructure
CCR = levelized annual capital carrying charge rate
MF = multiplication factor accounting for installation costs, construction, contingencies, etc.
p_{EL} = wholesale electricity price
h_{EQ} = number of full-load equivalent operating hours
t_{MIN} = lower bound to the temperature of a non-isothermal stream
t_{MAX} = upper bound to the temperature of a non-isothermal stream

Decision variables:
q_{ijk} = heat exchanged between hot stream i and cold stream j in stage k
$t_{i,k}$ = temperature of non-isothermal hot stream i at hot end of stage k
$t_{j,k}$ = temperature of non-isothermal cold stream j at hot end of stage k
dt_{ijk} = temperature approach for match (i,j) at temperature location k
z_{ijk} = binary variable to denote the activation of the match (i,j) in stage k
A_{ijk} = area of the heat exchanger between hot stream i and cold stream j in stage k

Constraints:
For the ones identified by *, only the formulation for hot streams is reported. An analogue one for cold streams can be easily obtained and is also present in the model.
Heat transfer direction:

$$q_{ijk} \geq 0 \quad \forall\, i \in I, j \in J, k \in K \qquad \text{Eq. (A.1)}$$

Energy balance for each process stream:

$$\left(T_{IN,i} - T_{OUT,i}\right) F_i c_{P,i} = \sum_{k \in K} \sum_{j \in J} q_{ijk} \quad \forall i \in I \cap P, i \notin ISO \quad *$$

$$F_i \lambda_i = \sum_{k \in K} \sum_{j \in J} q_{ijk} \quad \forall i \in I \cap P \cap ISO \quad * \qquad \text{Eq. (A.2)}$$

Energy balance for each "HEN utility" stream:

$$\left(T_{IN,i} - T_{OUT,i}\right) \dot{m}_i c_{P,i} = \sum_{k \in K} \sum_{j \in J} q_{ijk} \quad \forall i \in I \cap U, i \notin ISO \quad *$$

$$\dot{m}_i \lambda_i = \sum_{k \in K} \sum_{j \in J} q_{ijk} \quad \forall i \in I \cap U \cap ISO \quad * \qquad \text{Eq. (A.3)}$$

Energy balance of non-isothermal process streams in each stage:

$$\left(t_{ik} - t_{i,k+1}\right) F_i c_{P,i} = \sum_{j \in J} q_{ijk} \quad \forall i \in I \cap P, i \notin ISO \quad * \qquad \text{Eq. (A.4)}$$

Energy balance of non-isothermal "HEN utility" streams in each stage:

$$\left(t_{ik} - t_{i,k+1}\right) \dot{m}_i c_{P,i} = \sum_{j \in J} q_{ijk} \quad \forall i \in I \cap U, i \notin ISO \quad * \qquad \text{Eq. (A.5)}$$

Assignment of HEN superstructure inlet temperatures:

$$T_{IN,i} = t_{i,1} \quad \forall i \in I, i \notin ISO \quad * \qquad \text{Eq. (A.6)}$$

Monotonic temperature variation:

$$t_{i,k} \geq t_{i,k+1} \quad \forall i \in I, i \notin ISO, k \in K \quad *$$

$$T_{OUT,i} \leq t_{i,NOK+1} \quad \forall i \in I, i \notin ISO \quad * \qquad \text{Eq. (A.7)}$$

Logical constraints on the existence of heat exchangers:

$$q_{ijk} - \Omega_{ij} z_{ijk} \leq 0 \quad \forall i \in I, j \in J, k \in K \qquad \text{Eq. (A.8)}$$

Ω_{ij} is an upper bound for the heat which can be exchanged between the hot stream i and the cold stream j, it can be set to the smallest heat content of the two streams involved in the match.

Calculation of approach temperatures:

The following constraints are formulated for the left-hand side approach temperature differences (hot side):

$$dt_{ijk} \leq t_{i,k} - t_{j,k} + \Delta T_{MAX,ij}(1 - z_{ijk}) \quad \forall i \in I, j \in J, k \in K, i \notin ISO, j \notin ISO \qquad \text{Eq. (A.9)}$$

The following constraints concern the right-end side approach temperature differences (cold side):

$$dt_{ijk+1} \leq t_{i,k+1} - t_{j,k+1} + \Delta T_{MAX,ij}(1 - z_{ijk}) \quad \forall i \in I, j \in J, k \in K, i \notin ISO, j \notin ISO \qquad \text{Eq. (A.10)}$$

For the ISO streams, T_{IN} is used instead of t, generating four versions of each equation.
$\Delta T_{MAX,ij}$ is the upper bound for the approach temperature difference between hot stream i and cold stream j. Since excessively large values penalize the tightness of the problem formulation and damage the effectiveness of the optimization algorithm, $\Delta T_{MAX,ij}$ is set to the maximum value physically achievable in the HEN, i.e., the difference between the inlet temperature of hot stream i and the inlet temperature of the cold stream j. To avoid infinite areas, a positive lower bound $\mathcal{E}_{ij}$ can be specified for each approach temperature difference:

$$dt_{ijk} \geq \mathcal{E}_{ij} \qquad \forall i \in I, j \in J, k \in K \qquad \text{Eq. (A.11)}$$

"No-stream splitting" constraint:

$$\sum_{i \in I} z_{ijk} \leq 1 \quad \forall, j \in J, j \in SS, k \in K \quad * \qquad \text{Eq. (A.12)}$$

Forbidden matches:

$$z_{ijk} = 0 \quad \forall i \in I, j \in J, (i,j) \in FM, k \in K \qquad \text{Eq. (A.13)}$$

Restricted/required matches:

$$\sum_{k \in K} q_{ijk} \leq \dot{Q}_{MAX,ij} \quad \forall i \in I, j \in J, (i,j) \in RM$$

$$\sum_{k \in K} q_{ijk} \geq \dot{Q}_{MIN,ij} \quad \forall i \in I, j \in J, (i,j) \in RQ \qquad \text{Eq. (A.14)}$$

Activation/deactivation of utility streams:

The parameters $\dot{m}_{MAX,u}$ and $\dot{m}_{MIN,u}$ are respectively an upper and lower bound for mass flow rate of the u-th utility stream which must be set based on the problem specifications.

$$\dot{m}_u \leq y_u \dot{m}_{MAX,u} \quad \forall u \in U \qquad \text{Eq. (A.15)}$$

$$y_u \dot{m}_{MIN,u} \leq \dot{m}_u \quad \forall u \in U$$

Constraints for streams of the p-h superstructure:

$$\sum_{u \in U \cap IN_{he}} \dot{m}_u = \sum_{u \in U \cap OUT_{he}} \dot{m}_u \quad \forall\, he \in HE$$

$$\sum_{u \in U \cap IN_{he}} \dot{m}_u h_{OUT,u} = \sum_{u \in U \cap OUT_{he}} \dot{m}_u h_{IN,u} \quad \forall\, he \in HE \qquad \text{Eq. (A.16)}$$

Calculation of heat exchanger areas:

$$q_{ijk} \leq U_{ij} A_{ijk} \left(dt_{ijk} dt_{ijk+1} \frac{dt_{ijk} + dt_{ijk+1}}{2} \right)^{1/3} \quad \forall i \in I, j \in J, k \in K \qquad \text{Eq. (A.17)}$$

Logical constraints for heat exchanger areas:

$$A_{ijk} - A_{MAX,ij} z_{ijk} \leq 0 \quad \forall i \in I, j \in J, k \in K \qquad \text{Eq. (A.18)}$$

A_{MAX} is an upper bound for the heat which can be exchanged between the hot stream i and the cold stream j or between "HEN utility" streams and "end utilities". To obtain a tight problem formulation, A_{MAX} can be set as following:

$$A_{MAX,ij} = \frac{\Omega_{ij}}{U_{ij}\, \mathcal{E}_{ij}} \quad \forall i \in I, j \in J \qquad \text{Eq. (A.19)}$$

Objective function:

$$\begin{aligned} min\, TAC = CCR\, MF \Bigg(& \sum_{u \in U} C_{F,u} y_u + \sum_{i \in I} \sum_{j \in J} \sum_{k \in K} C_{F,ij} z_{ijk} \\ & + \sum_{u \in U, u \notin (I \cup J)} C_{S,u} S_{REF,u} \left(\frac{\dot{m}_u \Delta h_u}{S_{REF,u}} \right)^{\alpha_u} \\ & + \sum_{i \in I} \sum_{j \in J} \sum_{k \in K} F_{M,ij} F_{P,ij} C_{A,ij} A_{REF,ij} \left(\frac{A_{ijk}}{A_{REF,ij}} \right)^{\beta_{ij}} \Bigg) \\ & + \sum_{i \in I} C_{CU,i} q_{CU,i} + \sum_{j \in J} C_{HU\,j} q_{HU,j} \\ & - h_{EQ} p_{EL} \left(\sum_{u \in U \cap TURB} \dot{m}_u \Delta h_u - \sum_{r \in U \cap COMPR} \dot{m}_u \Delta h_u \right) \end{aligned} \qquad \text{Eq. (A.20)}$$

The expressions regarding HU and CU appear only in the objective function: they are referred to the utilities defined, at the beginning, as variable inlet/outlet utilities, such as cooling water or steam. In

all other aspects, as said, the concept of end utility has been removed. In the objective function, on the other hand, their cost is calculated considering their unit cost and flowrate.

The bare module cost of the heat exchanger between hot stream i and cold stream j is modeled with the following equation:

$$C_{HX,ijk} = F_{M,ij} F_{P,ij} C_{A,ij} A_{REF,ij} \left(\frac{A_{ijk}}{A_{REF,ij}} \right)^{\beta_{ij}} \quad \text{Eq. (A.21)}$$

where A_{ijk} is the heat exchanger area, F_M is the material factor (i.e. the ratio between the specific area cost of the material and that of carbon steel), which depends on the material employed (which in turn depends on the nature of the fluids and the temperatures, as specified in the material selection criteria described below), F_P is the pressure factor, which depends on the maximum pressure among the two fluids, $C_{A,ij}$ is the specific area cost at the reference area $A_{REF,ij}$, and β_{ij} is the scaling law exponent.

The investment cost for components of the utility superstructure is included in the objective function, typically related only to components like turbines, pumps, compressors. Considering a compressor in the p-h superstructure, since the inlet and outlet pressures and temperatures of the working fluid are fixed, the bare module cost of each compressor section is assumed to depend mainly on the size, S_u, of each component u (i.e., output power for turbines, input power for pumps, etc.) with an economy-of-scale effect given by:

$$C_u = C_{S,u} S_{REF,u} \left(\frac{S_u}{S_{REF,u}} \right)^{\alpha_u} \quad \text{Eq. (A.22)}$$

The total plant cost (TPC, i.e. total overnight installed cost of the HEN + utilities) is obtained by multiplying TBM by a multiplication factor (MF), also called Lang factor, that accounts for the installation costs, associated civil works, engineering and procurement, contingencies during construction and owners' costs.

The TPC is finally converted into a levelized annual cost via the capital carrying charge rate (CCR). The Total Annual Cost (TAC) is the sum of the annualized capital costs and the operating costs minus the revenue from selling electricity.

Appendix B: Model formulation with variable p and T of headers

Note that, since the model is built starting from the Fixed p and T of headers one, this formulation is presented, following the same structure, in terms of differences with respect to Fixed p and T of Headers version. Everything that is not found in Appendix B but is present in Appendix A is not modified and included in the new model in the same form as in Appendix A.

Additional sets:

IN_c = set of superstructure headers that enter component c

OUT_c = set of superstructure headers that exit component c

SC = set of sub-coolers

IC = set of intercoolers

SH = set of super-heaters

SEP = set of separators, subset of components in the p-h superstructure$varhe$ = set of variable headers

$varheLsat$ = set of saturated liquid superstructure headers

$varheVsat$ = set of saturated vapor superstructure headers

$varheSH$ = set of super-heated vapor superstructure headers

$varheSC$ = set of sub-cooled liquid superstructure headers

$varheM$ = set of two-phase superstructure headers

$varheCin$ = set of superstructure headers that enter a compressor

$varheCout$ = set of superstructure headers that exit a compressor

$varheIC$ = set of superstructure headers resulting from vapor mixing intercooling

$Plev$ = sets of headers that are part of the same pressure level, one set for each level

Additional decision variables:

$tvar$ = variable temperature of headers varhe

$hvar$ = variable enthalpy of headers varhe

$pvar$ = variable pressure of headers varhe

$svar$ = variable entropy of headers varhe

$tvar_{iso}$ = variable iso-entropic temperature of headers varhe. For compressors calculations

$hvar_{iso}$ = variable iso-entropic temperature of headers varhe. For compressors calculations

$thvar_{in}$ = variable inlet temperature of hot stream i

$thvar_{out}$ = variable outlet temperature of hot stream I

$hhvar_{in}$ = variable inlet enthalpy of hot stream I

$hhvar_{out}$ = variable outlet enthalpy of hot stream I

$tcvar_{in}$ = variable inlet temperature of cold stream J

$tcvar_{out}$ = variable outlet temperature of cold stream J

$hcvar_{in}$ = variable inlet enthalpy of cold stream J

$hcvar_{out}$ = variable outlet enthalpy of cold stream J

$hvar_{in}$ = variable inlet enthalpy of component stream C

$hvar_{out}$ = variable outlet enthalpy of component stream C

cph_{var} = variable Cp of hot stream I

cpc_{var} = variable Cp of cold stream J

Additional Constraints:

For the ones identified by *, only the formulation for hot streams is reported. An analogue one for cold streams can be easily obtained and is also present in the model

Enthalpy calculation:

The extrinsic functions require as inputs two properties to calculate the others. The total number of required inputs is equal to the number of components in the mixture plus two. First two inputs must be temperature and pressure, and the properties that can be calculated are enthalpy, entropy and fugacity. The inputs after the second are the molar fractions of the components of the mixture (=1 with pure refrigerants).

The result is divided by the molar weight because all the code is built referring to mass units while those functions are giving enthalpy and entropy on molar basis as output. The term A is used for rescaling. Two different expressions must be used because there are two different extrinsic functions for the calculation of each property: one for liquids and one from vapours. The appropriate one must be chosen for each header.

$$hvar = \frac{h_{liq}(tvar, pvar, 1)}{MW} + A \quad \forall\, he \in varheSC, varheLsat$$

$$hvar = \frac{h_{vap}(tvar, pvar, 1)}{MW} + A \quad \forall\, he \in varheVsat, varheSH, varheCout \qquad \text{Eq. (B.1)}$$

Entropy calculation:

The same considerations made for Eq. (2.21) can be made for entropy. Since values are positive and no comparison in needed, no modifications are made on the output given by the extrinsic functions.

$$svar = s_{vap}(tvar, pvar, 1) \quad \forall\, he \in varheCin$$

$$svar = s_{vap}(tvar_{iso}, pvar, 1) \quad \forall\, he \in varheCout \qquad \text{Eq. (B.2)}$$

Compressor's outlet conditions calculation:

To calculate the temperature and enthalpy at compressors outlet the definition of iso-entropic efficiency is used.

$$s_{comprIn} = s_{comprOut} \quad \forall\, COMPR$$

$$hvar_{iso} = \frac{h_{vap}(tvar_{iso}, pvar, 1)}{MW} + A \quad \forall\, he \in varheCout$$

$$h_{comprOut} = h_{comprIn} + \frac{h_{comprOutIso} - h_{comprIn}}{\eta_{iso}} \quad \forall\, COMPR \qquad \text{Eq. (B.3)}$$

Where:

$$
\begin{aligned}
s_{comprIn} &= \sum_{varheCin} svar \ \forall\, he \in IN_c, \forall\, COMP \\
s_{comprOut} &= \sum_{varheCout} svar \ \forall\, he \in OUT_c, \forall\, COMPR \\
h_{comprIn} &= \sum_{varheCin} hvar \ \forall\, he \in IN_c, \forall\, COMPR \\
h_{comprOut} &= \sum_{varheCout} hvar \ \forall\, he \in OUT_c, \forall\, COMPR \\
h_{comprOutIso} &= \sum_{varheCout} hvar_{iso} \ \forall\, he \in OUT_c, \forall\, COMPR
\end{aligned}
\qquad \text{Eq. (B.4)}
$$

Using these sums is a way to represent in the most general way the fact that for each property the value is taken equal to the one of the header entering/exiting the compressor, with a set division easy to handle inside the code. For each compressor in fact, the sum considers all possible inlets/outlets of compressors and choses the one respecting the given condition. For example, to calculate $s_{comprIn}$ the sum over the set of compressor inlet headers considers all possible inlets, considering just the one that is inlet to the chosen compressor, for each one of them.

This may seem redundant, but the alternative is to write the equations down individually, in a way that would need them to be re-written every time the code is run for a different cycle. This way, on the other hand, it's enough to modify the headers inside the sets when writing the new structure and the equations will work.

Saturation pressures calculation:

Pressure levels are calculated as saturation pressures of the temperatures of the various saturated liquid headers. Correlation used was Antoine's Equation; A, B and C represent the Antoine's coefficients for the selected fluid. Temperature is expressed in Celsius degrees. Depending on data availability different forms of Antoine's law were used in the work, so a conversion factor CONV is needed because pressures are always expressed in bar in the code and in all the results that will be shown. Mainly conversion resulted in division by 100 from kPa to bar and in multiplication by 0.00133322 from mmHg to bar. Also, in this second formulation exponential is not used with e basis but with 10 as basis, so the correct one between the shown equations is chosen depending on data availability.

$$
\begin{aligned}
pvar &= exp\left(A - \frac{B}{tvar + C} \right) * CONV \quad \forall\, he \in varheLsat \\
pvar &= 10^{\left(A - \frac{B}{tvar + C} \right)} * CONV \quad \forall\, he \in varheLsat
\end{aligned}
\qquad \text{Eq. (B.5)}
$$

Pressure and temperature levels definition:

For every pressure level saturation temperature and pressure are defined based on the saturated liquid relation. For this reason, pressures must be defined for the other headers of the level. Also, temperature is equal for saturated vapor and liquid.

$$tvar(varheLsat) = tvar(varheVsat) \quad \forall\, varheLsat, varheVsat \in Plev, \quad \forall\, Plev$$

$$pvar(varhe) = pvar(varheLsat) \quad \forall\, varhe, varheLsat \in Plev, \quad \forall\, Plev \qquad \text{Eq. (B.6)}$$

Two-phase headers enthalpy definition:

Two-phase headers enthalpy is defined starting from the output of the valve laminating to that header.

$$varhe = \sum_{VAL_{var}} hvar_{out} \;\forall\, VAL_{var} \in IN_{he}, \forall\, varhe \in varheM \qquad \text{Eq. (B.7)}$$

Sub-cooling conditions definition:

For the sub-cooled headers, temperature and enthalpy (related to each other by enthalpy calculation equations) must remain lower than the ones of the previous header (meaning the one that is input of the sub-cooled that has the calculated one as output) by a certain delta, taken equal to 1.

$$thvar_{out} \leq thvar_{in} + 1 \quad \forall\, U \in SC$$

$$hhvar_{out} \leq hhvar_{in} + 1 \quad \forall\, U \in SC \qquad \text{Eq. (B.8)}$$

Intercooling conditions definition:

For the headers coming from intercoolers, temperature and enthalpy (connected to each other by enthalpy calculation equations) must remain lower than the ones of the corresponding saturated liquid header by a certain delta, taken equal to 1.

$$thvar_{out} \leq thvar_{in} + 1 \quad \forall\, U \in IC$$

$$hhvar_{out} \leq hhvar_{in} + 1 \quad \forall\, U \in IC \qquad \text{Eq. (B.9)}$$

Super-heating conditions definition:

For the super-heating, temperature and enthalpy (connected to each other by enthalpy calculation equations) must be higher than the ones of the corresponding saturated vapor header by a certain delta, taken equal to 1.

$$thvar_{out} \geq thvar_{in} + 1 \quad \forall\, U \in SH \qquad \text{Eq. (B.10)}$$

$$hhvar_{out} \geq hhvar_{in} + 1 \quad \forall\, U \in SH$$

Vapor-mixing intercoolers limits definition:

The thermodynamic condition resulting from vapor mixing intercooler is intermediate in terms of temperature and pressure between saturated vapor and superheated header corresponding to the compressor outlet. Again, a minimum ΔT of 1° C is taken:

$$\begin{aligned}
&tvar(varheIC) \leq tvar(varheCout) - 1 \quad \forall\, varheCout, varheIC \in same\ Plev \\
&tvar(varheIC) \geq tvar(varheVsat) + 1 \quad \forall\, varheVsat, varheIC \in same\ Plev \\
&hvar(varheIC) \leq hvar(varheCout) - 1 \quad \forall\, varheCout, varheIC \in same\ Plev \\
&hvar(varheIC) \geq hvar(varheVsat) + 1 \quad \forall\, varheVsat, varheIC \in same\ Plev
\end{aligned} \qquad \text{Eq. (B.11)}$$

Definition of inlet/outlet temperatures and enthalpies of streams:

A different expression is needed for each one of the various streams available in the structure, since the headers properties vary at each iteration:

- Hot and cold streams: temperature and enthalpy are defined as inlet and outlet headers properties
- Valves: keep enthalpy constant, equal to the inlet one
- Compressors: outlet and inlet enthalpies are defined as outlet/inlet headers properties
- Separators: the two separated streams keep enthalpy constant, equal to the one of their outlets. This way it is modelled separation of saturated liquid and vapor.

For hot and cold streams both temperatures and enthalpies must be defined, since they are both needed for heat exchange calculations. On the other hand, just constraints on enthalpy are needed for the other components, since temperature is just needed for exchangers' areas calculations.

The same concept about the sums used for compressors properties is applied here: this way of writing is used for generalization reasons, otherwise it would be necessary to rewrite the corresponding equations every time the structure is modified (e.g. adding or removing pressure levels, adding or removing super-heating…).

$$thvar_{in} = \sum_{varhe} tvar \ \forall\, he \in IN_c, \forall\, I \ *$$

$$thvar_{out} = \sum_{varhe} tvar \ \forall\, he \in OUT_c, \forall\, I \ *$$

$$hhvar_{in} = \sum_{varhe} hvar \ \forall\, he \in IN_c, \forall\, I \ *$$

$$hhvar_{out} = \sum_{varhe} hvar \ \forall \ he \in OUT_c, \forall \ I \quad * \qquad \text{Eq. (B.12)}$$

$$hvar_{in} = \sum_{varhe} hvar \ \forall \ he \in IN_c, \forall \ VALVE, COMPR$$

$$hvar_{in} = \sum_{varhe} hvar \ \forall \ he \in OUT_c, \forall \ SEP$$

$$hvar_{out} = hvar_{in} \ \forall \ VALVE, SEP$$

$$hvar_{out} = \sum_{varhe} hvar \ \forall \ he \in OUT_c, \forall \ COMPR$$

Definition of c_p for hot/cold streams of the HEN:

For the isothermal streams, the enthalpy of evaporation or condensation is considered while for the non-isothermal streams the mean specific heat capacity at constant pressure is calculated as the ratio between the enthalpy difference from the inlet to the outlet headers (Δh) and the temperature difference ΔT.

$$cph_{var} = \frac{hhvar_{in} - hhvar_{out}}{thvar_{in} - thvar_{out}} \quad \forall \ I \notin ISO \quad * \qquad \text{Eq. (B.13)}$$

$$cph_{var} = hhvar_{in} - hhvar_{out} \ \forall \ I \in ISO \quad *$$

This approach of defining the mean c_p guarantees that the total energy balance of the hot and cold streams is met when integrating the cycle superstructure model with the HEN superstructure model.

Modified Constraints:

All the equations involving utility streams (and so T and p) of Appendix A must be doubled because of the difference between variable and fixed streams; for each one of them another one is written, identical but using the newly defined variables as thermodynamic properties instead of the parameters for the headers defined as variable in set varhe. Clearly, if some headers are left fixed, their properties need to remain defined as parameters. Thanks to the double formulation of the constraints, the model is flexible and both fixed and variable headers can be defined at the same time. This doubling is important because:

- Being able to choose between fixed and variable headers makes the code more versatile
- Even when all the structure varies, some headers/flows may need to remain constant, for instance the utility headers (e.g. water for cooling and steam for heating): their inlet/outlet is already variable for definition, but inlet and outlet headers thermodynamic conditions should remain still.

References

[1] A. S. Wallerand, M. Kermani, I. Kantor, and F. Maréchal, "Optimal heat pump integration in industrial processes," *Appl. Energy*, vol. 219, pp. 68–92, 2018, doi: 10.1016/j.apenergy.2018.02.114.

[2] A. Alabdulkarem, Y. Hwang, and R. Radermacher, "Development of CO2 liquefaction cycles for CO2 sequestration," *Appl. Therm. Eng.*, vol. 33–34, pp. 144–156, 2012, doi: 10.1016/j.applthermaleng.2011.09.027.

[3] S. S. Baakeem, J. Orfi, and A. Alabdulkarem, "Optimization of a multistage vapor-compression refrigeration system for various refrigerants," *Appl. Therm. Eng.*, vol. 136, pp. 84–96, 2018, doi: 10.1016/j.applthermaleng.2018.02.071.

[4] Nasruddin, S. Sholahudin, N. Giannetti, and Arnas, "Optimization of a cascade refrigeration system using refrigerant C3H8 in high temperature circuits (HTC) and a mixture of C2H6/CO2 in low temperature circuits (LTC)," *Appl. Therm. Eng.*, vol. 104, pp. 96–103, 2016, doi: 10.1016/j.applthermaleng.2016.05.059.

[5] S. Eini, H. Shahhosseini, N. Delgarm, M. Lee, and A. Bahadori, "Multi-objective optimization of a cascade refrigeration system: Exergetic, economic, environmental, and inherent safety analysis," *Appl. Therm. Eng.*, vol. 107, pp. 804–817, 2016, doi: 10.1016/j.applthermaleng.2016.07.013.

[6] M. R. Shelton and I. E. Grossmann, "Optimal synthesis of integrated refrigeration systems-I. Mixed-integer programming model," *Comput. Chem. Eng.*, vol. 10, no. 5, pp. 445–459, 1986, doi: 10.1016/0098-1354(86)85014-1.

[7] M. R. Shelton and I. E. Grossmann, "Optimal synthesis of integrated refrigeration systems-II. Implicit enumeration scheme," *Comput. Chem. Eng.*, vol. 10, no. 5, pp. 461–477, 1986, doi: 10.1016/0098-1354(86)85015-3.

[8] F. Marechal and B. Kalitventzeff, "A tool for optimal synthesis of industrial refrigeration systems," *Comput. Aided Chem. Eng.*, vol. 9, pp. 457–462, 2001, doi: 10.1016/S1570-7946(01)80071-7.

[9] M. M. F. Hasan, M. S. Razib, and I. A. Karimi, "Optimization of Compressor Networks in LNG Operations," in *Computer Aided Chemical Engineering*, 2009, pp. 1767–1772.

[10] M. Kamalinejad, M. Amidpour, and S. M. M. Naeynian, "Thermodynamic design of a cascade refrigeration system of liquefied natural gas by applying mixed integer non-linear programming," *Chinese J. Chem. Eng.*, 2015, doi: 10.1016/j.cjche.2014.05.023.

[11] B. Ghorbani, G. R. Salehi, H. Ghaemmaleki, M. Amidpour, and M. H. Hamedi, "Simulation and optimization of refrigeration cycle in NGL recovery plants with exergy-pinch analysis," *J. Nat. Gas Sci. Eng.*, 2012, doi: 10.1016/j.jngse.2012.03.003.

[12] T. Yang, Y. Luo, Y. Ma, and X. Yuan, "Optimal synthesis of compression refrigeration system using a novel MINLP approach," *Chinese J. Chem. Eng.*, 2018, doi: 10.1016/j.cjche.2017.10.028.

[13] B. J. Zhang, Z. L. Zhang, K. Liu, and Q. L. Chen, "Network Modeling and Design for Low Grade Heat Recovery, Refrigeration, and Utilization in Industrial Parks," *Ind. Eng. Chem. Res.*, 2016, doi: 10.1021/acs.iecr.6b02033.

[14] G. Oluleye, M. Jobson, and R. Smith, "Process integration of waste heat upgrading technologies," *Process Saf. Environ. Prot.*, 2016, doi: 10.1016/j.psep.2016.02.003.

[15] C. J. King and F. J. Barnés, "Synthesis of Cascade Refrigeration and Liquefaction Systems," *Ind. Eng. Chem. Process Des. Dev.*, vol. 13, no. 4, pp. 421–433, 1974, doi: 10.1021/i260052a022.

[16] T. R. Colmenares and W. D. Seider, "Synthesis of cascade refrigeration systems integrated with chemical processes," *Comput. Chem. Eng.*, 1989, doi: 10.1016/0098-1354(89)85002-1.

[17] S. Vaidyaraman and C. D. Maranas, "Optimal synthesis of refrigeration cycles and selection

of refrigerants," *AIChE J.*, vol. 45, no. 5, pp. 997–1017, 1999, doi: 10.1002/aic.690450510.
[18] H. Dinh, J. Zhang, and Q. Xu, "Process synthesis for cascade refrigeration system based on exergy analysis," *AIChE J.*, 2015, doi: 10.1002/aic.14843.
[19] C. Elsido, E. Martelli, and I. E. Grossmann, "A bilevel decomposition method for the simultaneous heat integration and synthesis of steam/organic Rankine cycles," *Comput. Chem. Eng.*, 2019, doi: 10.1016/j.compchemeng.2019.05.041.
[20] C. Elsido, E. Martelli, and I. E. Grossmann, "Multiperiod optimization of heat exchanger networks with integrated thermodynamic cycles and thermal storages," *Comput. Chem. Eng.*, vol. 149, p. 107293, 2021, doi: 10.1016/j.compchemeng.2021.107293.
[21] T. F. Yee and I. E. Grossmann, "Simultaneous optimization models for heat integration-II. Heat exchanger network synthesis," *Comput. Chem. Eng.*, vol. 14, no. 10, pp. 1151–1164, 1990, doi: 10.1016/0098-1354(90)85010-8.
[22] C. Elsido, A. Mian, and E. Martelli, "A systematic methodology for the techno-economic optimization of Organic Rankine Cycles," *Energy Procedia*, vol. 129, pp. 26–33, Sep. 2017, doi: 10.1016/j.egypro.2017.09.171.
[23] C. Elsido, A. Mian, F. Marechal, and E. Martelli, "A general superstructure for the optimal synthesis and design of power and inverse Rankine cycles," in *Computer Aided Chemical Engineering*, 2017, pp. 2407–2412.
[24] J. I. Manassaldi, M. C. Mussati, N. J. Scenna, and S. F. Mussati, "Development of extrinsic functions for optimal synthesis and design—Application to distillation-based separation processes," *Comput. Chem. Eng.*, vol. 125, pp. 532–544, 2019, doi: 10.1016/j.compchemeng.2019.03.028.
[25] J. I. Manassaldi, M. C. Mussati, N. J. Scenna, and S. F. Mussati, "User's manual to use thermodynamic libraries in GAMS through extrinsic functions," [Online]. Available: https://www.gams.com/community/contributed-software/.
[26] E. Martelli, C. Elsido, A. Mian, and F. Marechal, "MINLP model and two-stage algorithm for the simultaneous synthesis of heat exchanger networks, utility systems and heat recovery cycles," *Comput. Chem. Eng.*, vol. 106, pp. 663–689, 2017, doi: 10.1016/j.compchemeng.2017.01.043.
[27] J. J. J. Chen, "Comments on improvements on a replacement for the logarithmic mean," *Chem. Eng. Sci.*, vol. 42, no. 10, pp. 2488–2489, 1987, doi: 10.1016/0009-2509(87)80128-8.
[28] G. P. McCormick, "Computability of global solutions to factorable nonconvex programs: Part I - Convex underestimating problems," *Math. Program.*, 1976, doi: 10.1007/BF01580665.
[29] IBM ILOG CPLEX, "CPLEX v.12.8, mathematical programming solver," [Online]. Available: https://www.ibm.com/analytics/cplex-optimizer.
[30] M. Tawarmalani and N. V. Sahinidis, "A polyhedral branch-and-cut approach to global optimization," *Math. Program.*, vol. 103, no. 2, pp. 225–249, 2005, doi: 10.1007/s10107-005-0581-8.
[31] Z. Ugray, L. Lasdon, J. C. Plummer, and M. Bussieck, *Dynamic filters and randomized drivers for the multi-start global optimization algorithm MSNLP*, vol. 24, no. 4–5. 2009.
[32] A. Drud, "CONOPT: A GRG code for large sparse dynamic nonlinear optimization problems," *Math. Program.*, vol. 31, pp. 153–191, 1985, doi: 10.1007/BF02591747.
[33] A. S. Drud, "CONOPT—A Large-Scale GRG Code," *ORSA J. Comput.*, vol. 6, pp. 207–216, 1994, doi: 10.1287/ijoc.6.2.207.
[34] G. Xu, F. Liang, Y. Yang, Y. Hu, K. Zhang, and W. Liu, "An improved CO2 separation and purification system based on cryogenic separation and distillation theory," *Energies*, vol. 7, pp. 2484–2502, 2014, doi: 10.3390/en7053484.